**Vehicle Development Technology**

Report No. AVET-84-02

DATE February 20, 1984

## PROJECT REPORT

TO: Mr. R. E. VanHouse

cc: See attached Distribution List 2004

SUBJECT: Static Geometric and Material Non-Linear Analysis of an S-Frame Using MSC/NASTRAN 7-1-1

### Purpose

This series of analyses was conducted to assess the capability of MSC/NASTRAN, Version 61B, to perform a static non-linear analysis of an automotive component undergoing large displacements and having non-linear material properties. The problem chosen was that of a symmetric S-frame under static crush loading (see Figure 1). Results from physical tests (Figure 2) and also from competitive analysis programs can be found in the references, and were used to judge the validity of the MSC/NASTRAN results. Because of the estimated cost to perform the testing, the physical test data was taken from SAE Paper 770614 (Reference #1).

MSC/NASTRAN is Ford's principle structural analysis program for the linear analysis of vehicle components. Its ease of use and capability to perform non-linear analysis has never been demonstrated. For non-linear problems (i.e. elasto-plastic analysis for fatigue and limit analysis, large displacement analysis for kinematics, and coupled elasto-plastic and large displacement for crush performance), a number of other programs are being used, some that are developed and maintained by consulting firms, others that are being developed by Ford personnel.

If it would be possible to standardize on a single analysis program, productivity and cost improvements could be realized in the following areas:

- Reduce or eliminate cost for development and support of redundant programs.
- Analysis model pre-and-post processing software development and support.
- Applications to automotive testing and development methods.
- Training of engineers in how to use the program.

The project described in this report was to see how close MSC/NASTRAN would predict real-world crush performance for the initial deformations, up to and slightly beyond the development of a maximum simulated barrier force (approximately 18,000 pounds of barrier force at a crush distance of about .6 of an inch). Once MSC/NASTRAN has shown to be capable of predicting the maximum barrier force, at the correct crush distance, and with accurate energy absorption measures, the intent is to continue, and document in a subsequent report, the performance prediction to at least 6 inches of crush.

Pending successful completion of the non-linear static analysis, dynamic effects could be included using a newly-released capability of MSC/NASTRAN.

### Results

The MSC/NASTRAN S-frame model predicts the following:

- With elastic-perfect plastic material description, the simulated barrier forces are greater than test in the initial part of the curves.

Results (continued)

- With 36,000 psi yield material assumed, the maximum predicted barrier force is less than test results and occurs at a lower value of crush distance.

- The barrier force versus crush distance curves are insensitive to varying small values of plastic modulus.

- The barrier force versus crush distance curves are very sensitive to varying large values of plastic modulus.

- Correlation with an elastic-perfect plastic model can be improved for small values of crush distance by a downward adjustment of Young's modulus.

- Correlation for larger values of crush distance can be improved by an upward adjustment of the VonMises yield stress.

- In either of the above adjustments, the moderate crush distance correlation shows significant deviation of analysis from test.

- Using an elastic-perfect plastic material description with a "fine" model does not improve correlation.

- Boundary condition changes at the simulated barrier face can be used to improve analysis correlation, but cannot be justified, based on the description of the test in the published SAE paper (Reference 1).

- Correlation improves dramatically when a table of stress/strain information can be obtained for the material from which the S-frame was constructed.

In summary, when an accurate material description is submitted to MSC/NASTRAN in the form of material property and stress/strain table cards, the predicted barrier force as a function of crush distance is in excellent agreement to that of the published test results (see Figure 3).

Conclusion

In order to perform this type of analysis, an accurate description of the material properties is required. The accuracy of this material description may be more important than the detail of the finite element model or of the accuracy of the load and boundary conditions. The material description used in this analysis was a stress/strain table derived from material samples, and tabulated as part of the Ford Scientific Research Materials Data Base, developed by Drs. Landgraf and Conle (see Figures 4, 5, and 6 for sample graphs).

Recommendations

Since completing this series of analyses, MSC has released a new solution sequence, Solution 99 - Dynamic Geometric and Material Non-Linearity. The subject problem should be converted to this dynamic solution, and new performance measures developed.

Due to cost and time constraints, the crush performance of the S-frame was only tabulated to .6 of an inch of overall crush. The problem should be extended to at least 6 inches or more of crush.

Finally, using the same model, boundary conditions and material properties that proved so successful in this analysis, the performance of other non-linear programs could be investigated.

Mark P. Zebrowski

Mark P. Zebrowski

Concur: N. Baracos

N. Baracos, Manager

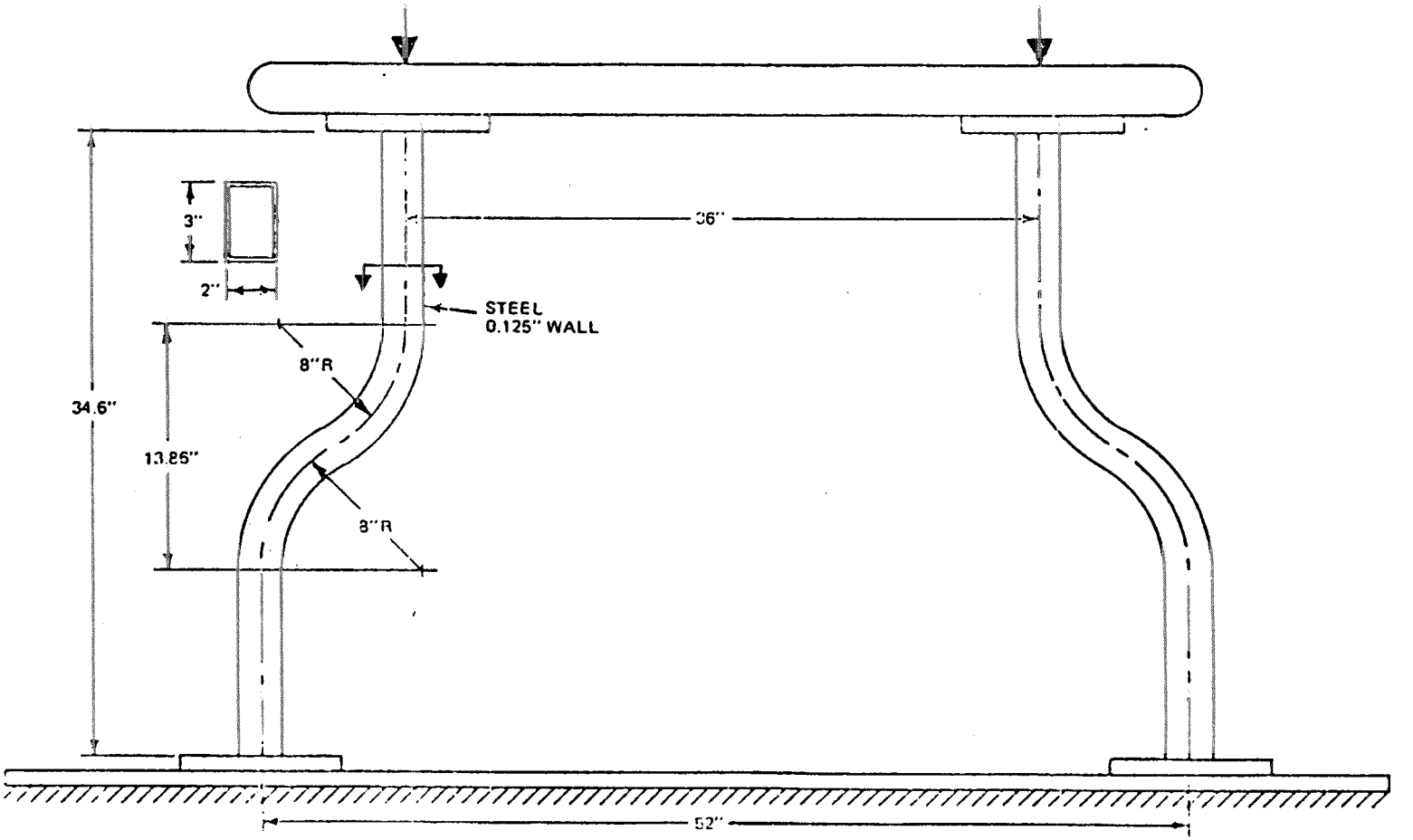


Figure 1 - S-Frame undergoing static crush.

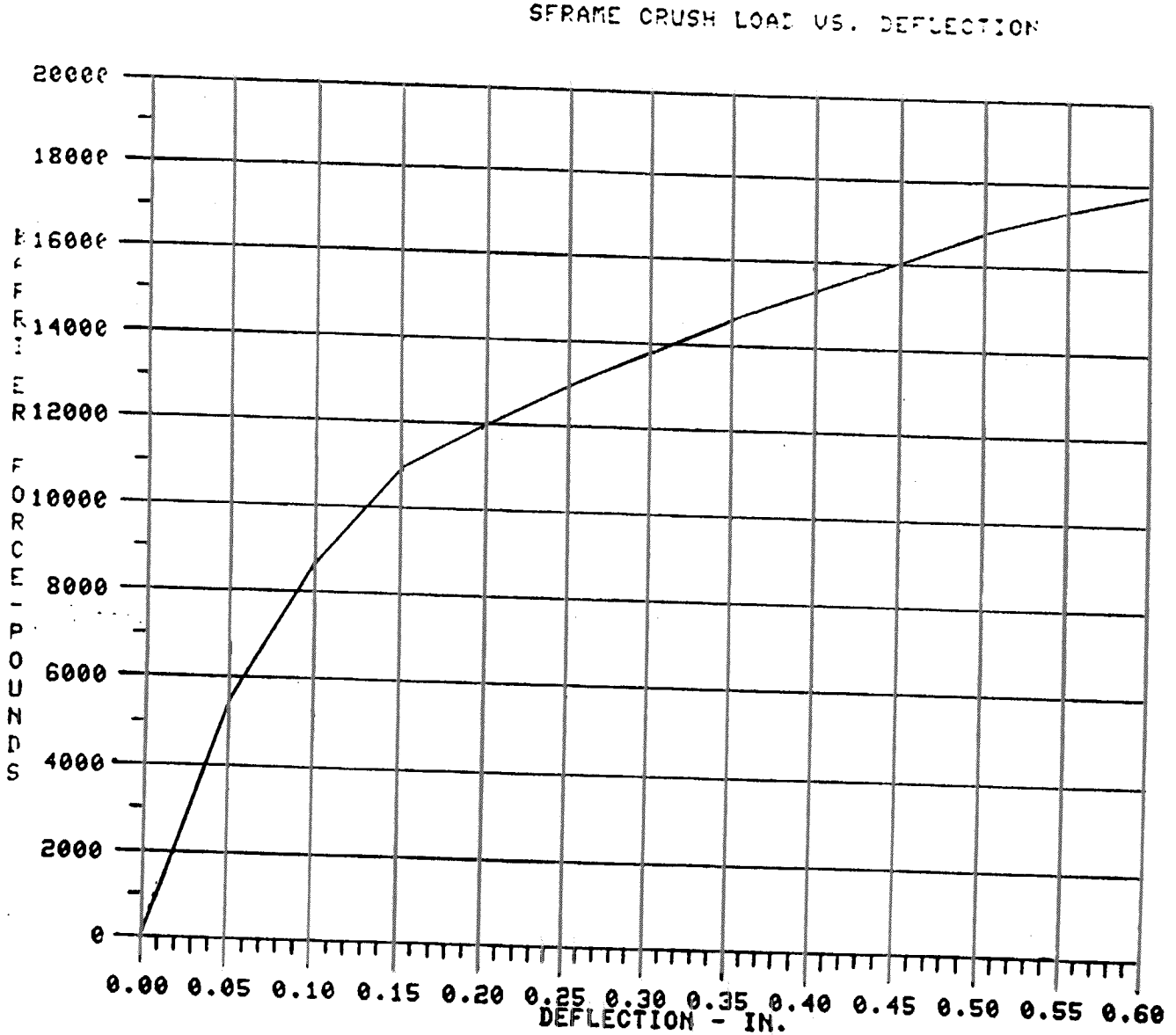


Figure 2 - Barrier force versus crush distance (testing completed at General Motors and taken from SAE 776014).

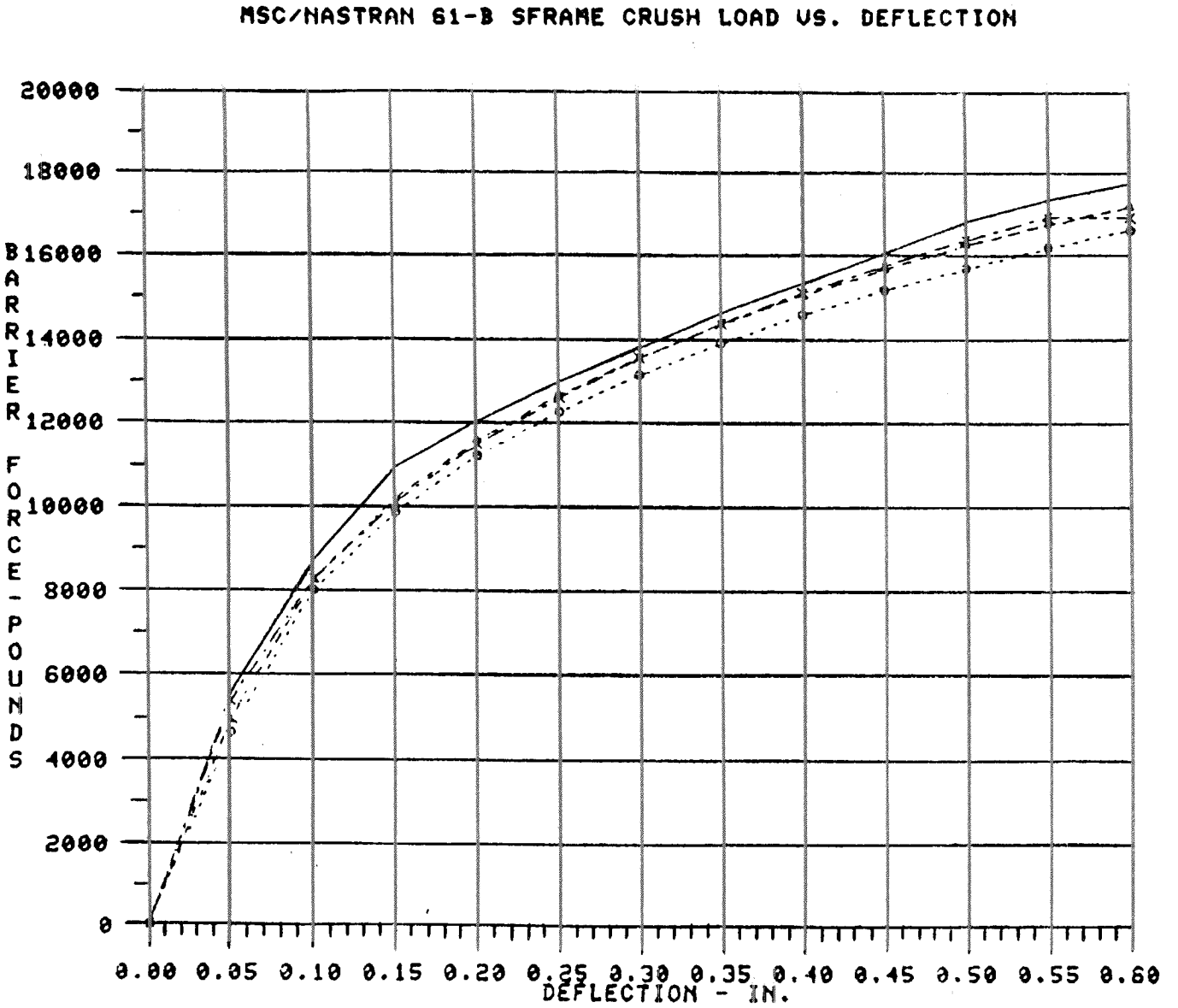


Figure 3 - Final results comparing published test results with simulations using 3 different SAE 1006

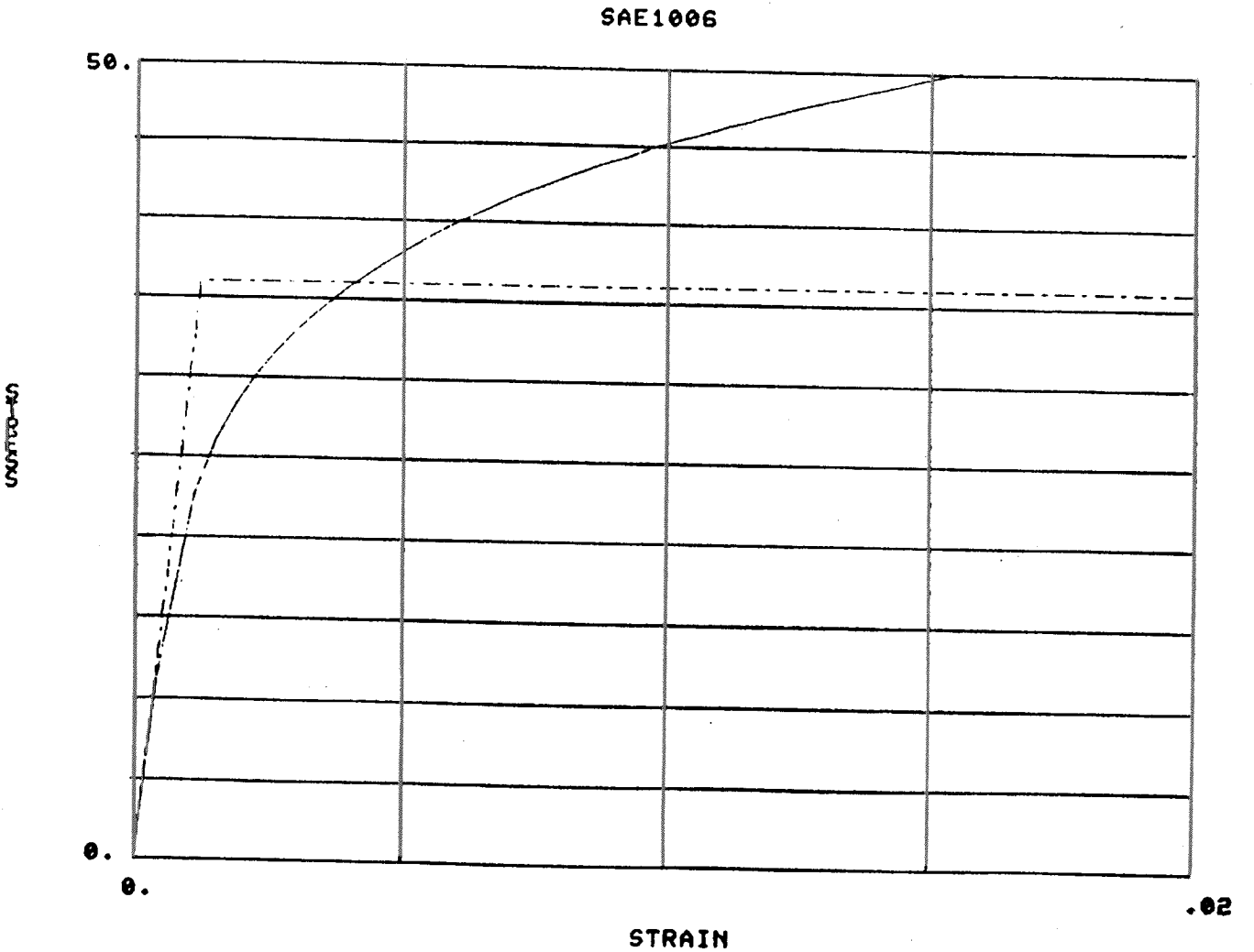


Figure 4 - Stress versus strain for materials' file number 75.

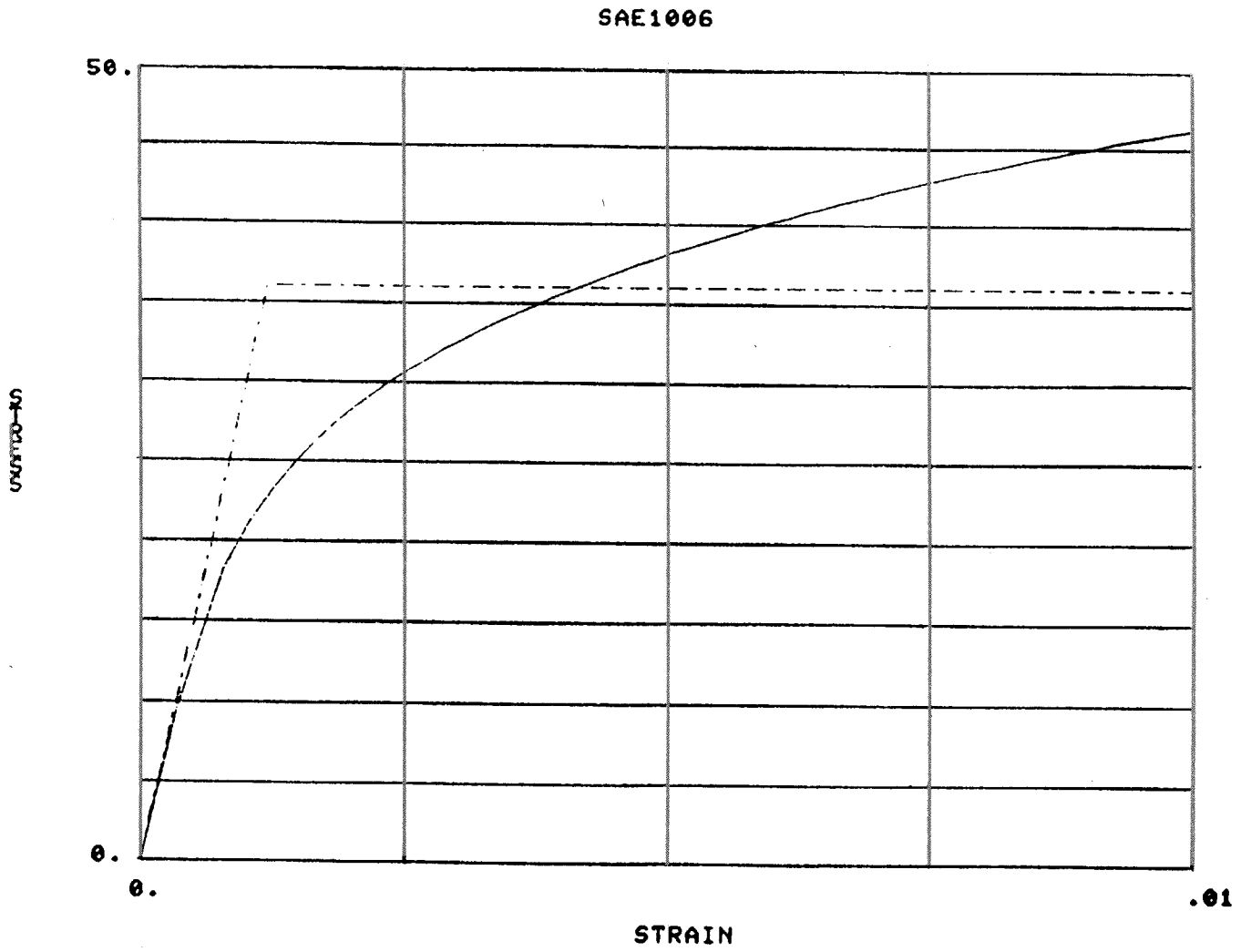


Figure 5 - Stress versus strain for materials' file number 77.

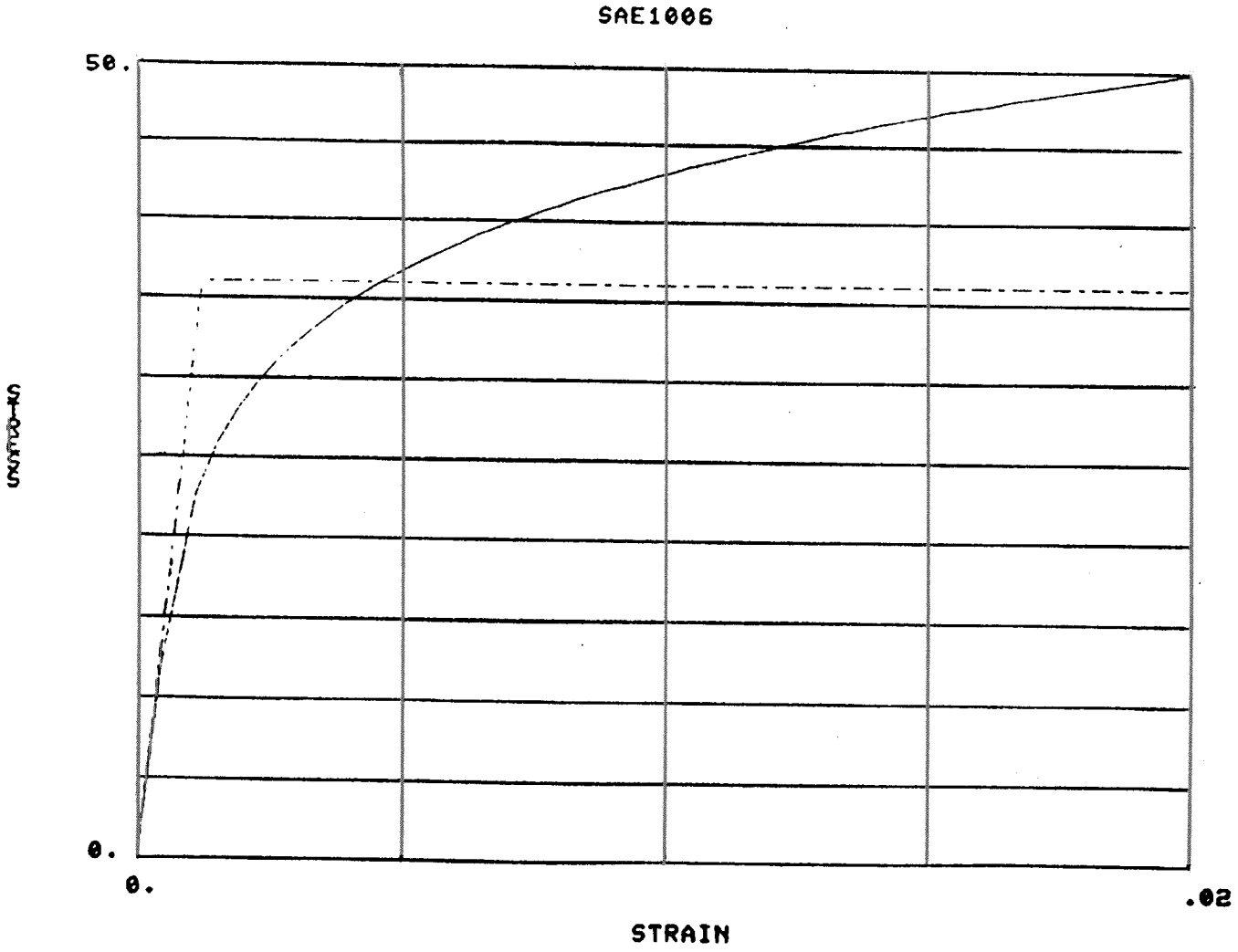


Figure 6 - Stress versus strain for materials' file number 78.

Ford Experiences with Non-Linear MSC/NASTRAN

MSC/NASTRAN has had the capability of solving geometric and material non-linear problems for many years. One of the first series of non-linear MSC/NASTRAN analyses was completed here at Ford by Mr. Steward J. Lammers, formerly of the Engineering Methods and Applications Department of Product Planning and Research, currently with the Taurus Platform Program Control and Design Services Department of the Car Product Development Group. Mr. Lammers used the Piecewise Linear capability (Rigid Format Solution Number 6) of MSC/NASTRAN Version 23 (October 1, 1974 release date) to refine the boundary conditions near bolted joints and where parts, under certain loading directions, bear up against or pull away from other attaching parts (see Figures 7 and 8). The capability, although satisfactory at the time, became technically obsolete in the latter part of the '70's, in relation to other finite element programs. MSC/NASTRAN was known, primarily, as a linear finite element system.

In 1976, a modernized geometric non-linear capability was released in the form of a DMAP (Direct Matrix Abstraction Programming) sequence, DMAP4. The author and Mr. Don Mikulec used this new capability in the loads analysis of a 1979 Ford prototype, running over a "North Dakota Square Edge Pothole", part of the P322D durability test (see Figure 9). The body and frame structures' dynamic character were idealized as a set of multipoint constraint equations (MPC's), synthesized from 1979 Ford body and frame superelement model mode shapes. The front and rear suspensions were modeled with beam and spring elements, with concentrated inertias simulating powertrain components. DMAP4 was a large displacement linear material static analysis capability. This required that the system of body, frame, and powertrain and chassis components be constrained. The choice was made to constrain the translational rigid body modes of the body structure. High-speed photographic motion pictures were made, and the digitized displacements of the wheel center were imposed on the analytic system model. Body mount loads from the test were compared to the analysis predictions. Numerous other applications of DMAP4 were attempted, but most of them were of an academic nature. The FORD NASTRAN Users' Group made a study of the buckling characteristics of a square tube with a central notch, using all available solutions -- Solution 5, DMAP1 with a restart in DMAP5, and DMAP4 (see Figure 10). Also, cable routing problems were solved using DMAP4 and compared to closed form solutions, when these solutions were available.

When the new solution procedure combining geometric non-linearity with material non-linearity was released as Solution 66, Dr. R. Narayan Swami, an MSC/NASTRAN consultant located in Northridge, California, was brought to Ford where he taught a five-day course in October, 1981 on Solutions 64 and 66. The course material displayed the capabilities of the new solutions and reviewed the underlying engineering theory. A number of small sample problems were solved in that class, most successfully, some with varying degrees of success. However, when attempts were made to apply the methods to real-life problems, numerous difficulties arose. The most significant applications were to frame crush (documented in this report), Belleville clutch performance, and fuel filler flapper valve analysis. In general successful completion of a non-linear production analysis only resulted when the analyst approached the problem as a personal challenge. It was not unusual for a practical problem with mild non-linearities to be ten to one hundred times more costly and time-consuming than a related static analysis, making some simplifying assumptions.

Frame crush analysis is documented in this VDT report; the Belleville clutch performance analysis, completed by Mr. George Campbell of Light Truck Design

1 11/18/74 1

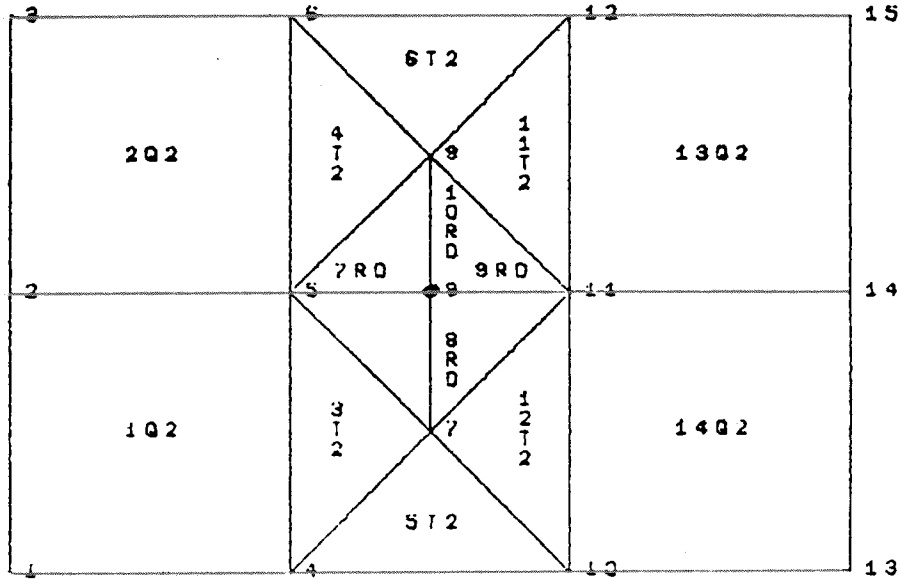


SAMPLE PROBLEM PIECE-WISE LINEAR ANLYSIS
PLATE WITH HOLE IN CENTER - FIXED AT CENTER OF HOLE

UNDEFORMED SHAPE

Figure 7 - Finite Element model to analyze bearing load at a bolted joint.

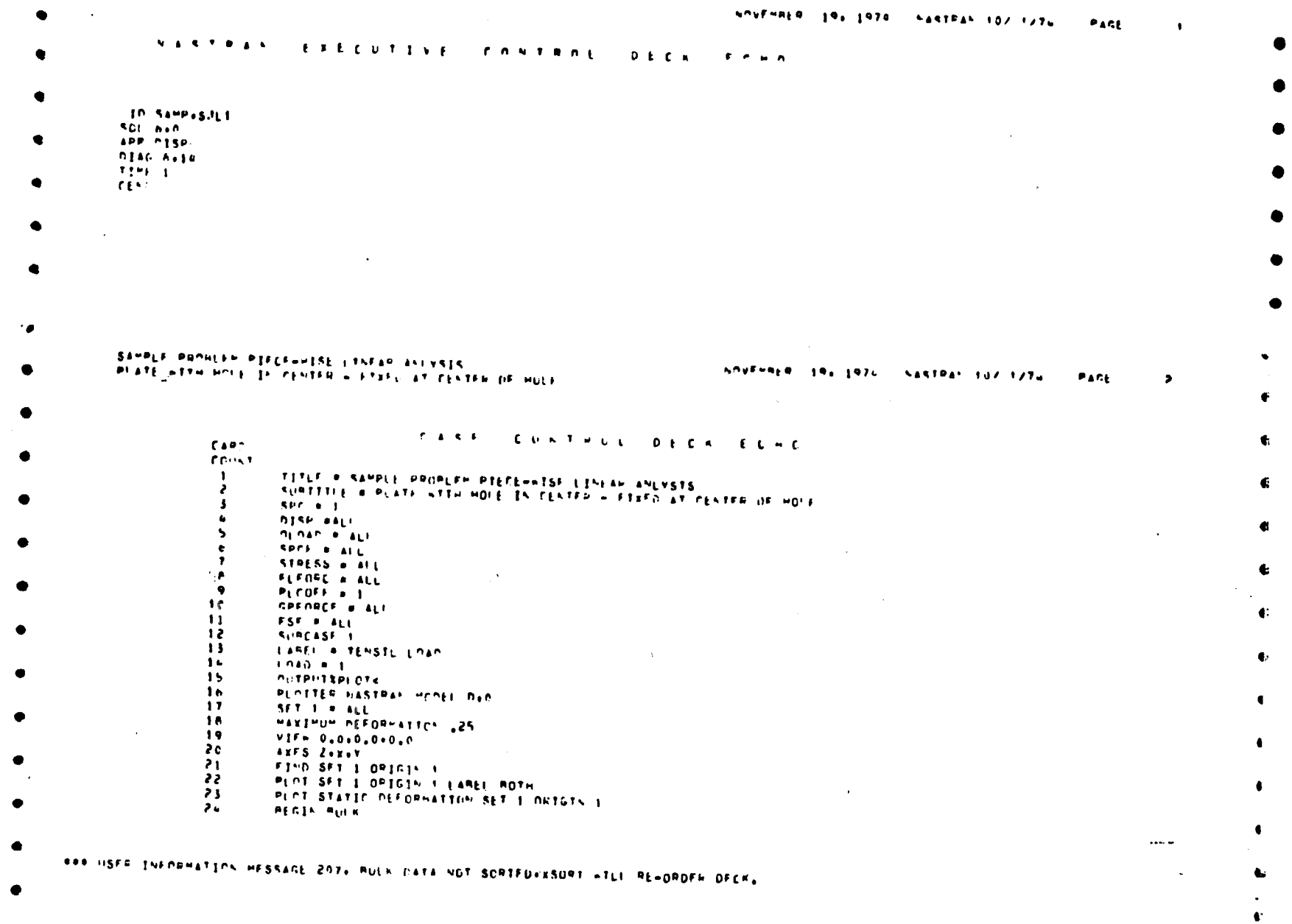


Figure 8 - MSC/NASTRAN executive and case control
for piecewise linear analysis (Solution 6).

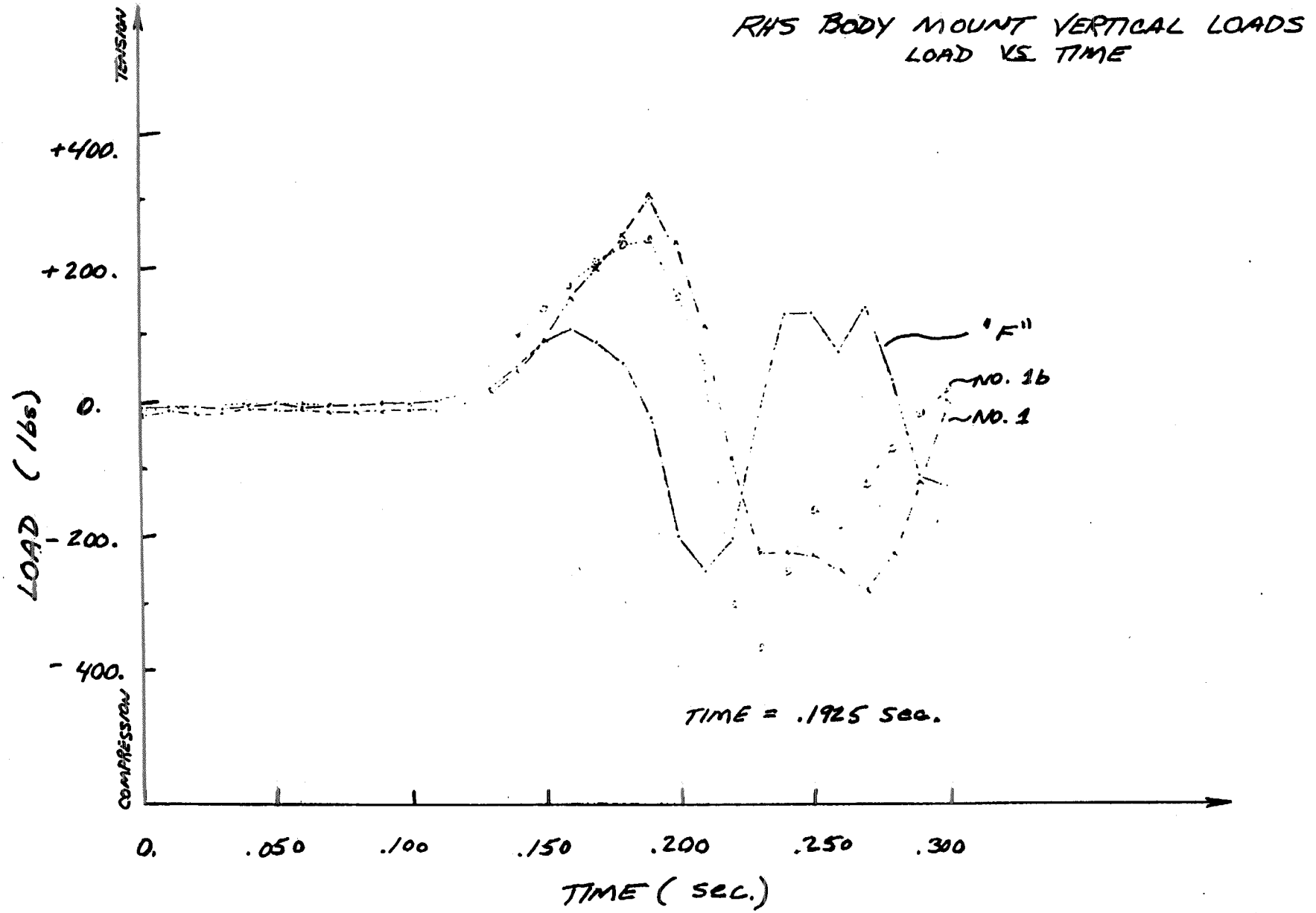


Figure 9 - Simulate body mount loads for the Pothole Event of P322D.

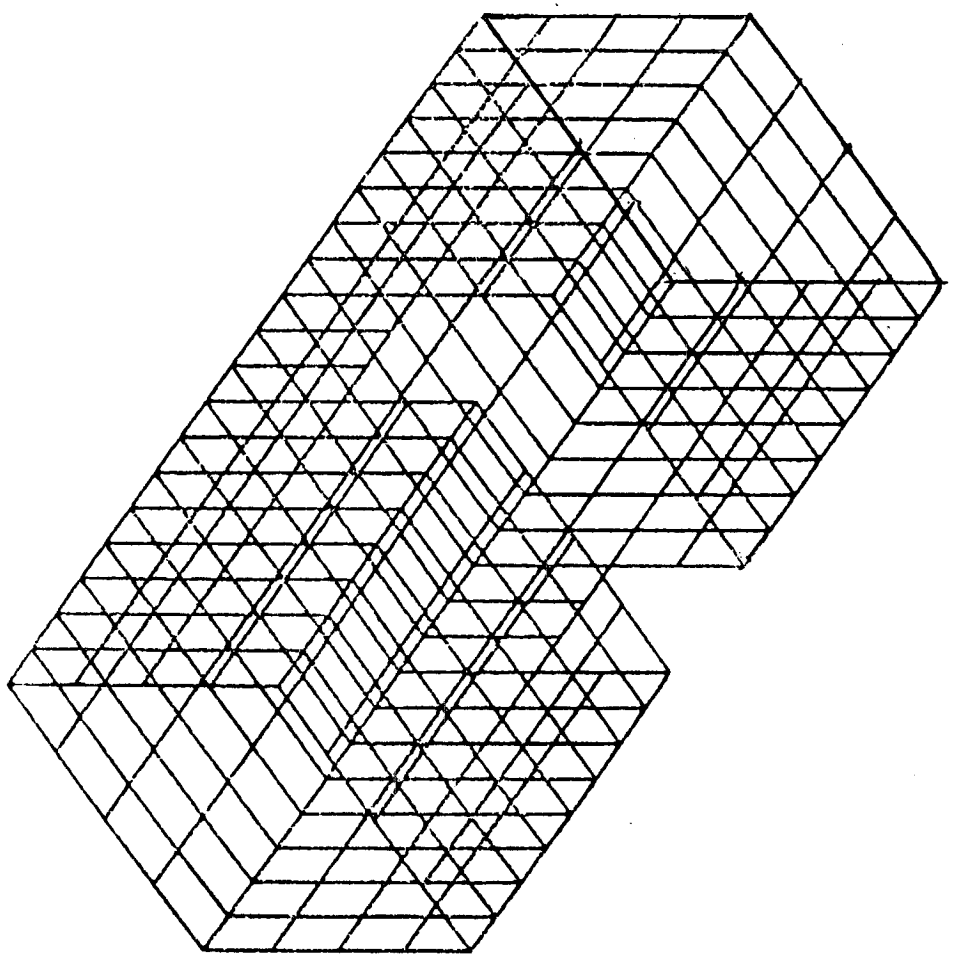

Figure 10 - Square tube with central notch.

Analysis, and the fuel filler flapper valve problem, analyzed by Mr. James Brancheau - also of Light Truck Design Analysis - have been reported in Light Truck Engineering program reports (see References 5 & 6).

The most difficult problem has been that of constraining singularities normal to a plate (CQUAD4 or CTRIA3 elements) surface, and has been solved, with difficulty, by a variety of methods: with an application of single-point constraints (SPC's); with a net of beams (CBEAM's); with linear rotational springs (CELAS's) to ground; etc. Each of the previously-mentioned applications required a different approach to the treatment of these singularities. The S-frame problem has an undeformed shape where normal rotations are singular. The Belleville clutch deforms into a shape where normal rotations are singular. The fuel filler flapper valve displaces through approximately 90° of rigid body motion, so singularities due to normal rotations could develop twice -- at the beginning and end of motion -- and could develop about two different global axes. MSC has promised to remove these difficulties and make non-linear analysis more user-friendly by modifying the stiffness of the plate elements by adding a small spring rate to the element stiffness matrix. This modification to MSC/NASTRAN will be a great help.

The S-frame problem documented in this report was first attempted - using MSC/NASTRAN - at Ford by Dr. Heng Yee Chen of the Advanced Vehicle Structures and Safety Engineering Department of the Body and Electrical Product Engineering Office. In October, 1981 the problem was discussed as part of Dr. R. Narayan Swami's non-linear course and, in November, Dr. Heng Yee Chen presented his results to the Ford NASTRAN Users' Group. His approach to the initial singularities in this problem was to use the Grid Point Singularity Processor, Phase 1 (GPSP1) module of linear static analysis, Solution 24, to produce a set of single point constraints to be applied to the model. The difficulty with this approach is that degrees of freedom that are initially singular may not remain so under large deformation loadings. His results indicated that the added singularity constraints were artificially constraining the structure. The simulated barrier force continuously increased as a function of increasing crush distance. The test results indicated the barrier force reaches a maximum near .6 of an inch of crush, then drops off. The consensus of the meeting attendees was that this problem, along with that of the Belleville clutch that Light Truck was analyzing and experiencing considerable difficulty with, was to be submitted to the MacNeal-Schwendler analysts. MSC was commissioned to solve both problems and report back to the Users' Group during MSC's quarterly visit to Ford, scheduled for January of 1982. MSC analysts, working together with Ford personnel, reported in their January visit that major modeling and programming difficulties had been resolved, and that both problems were now giving reasonable results. Parametric studies of both the S-Frame and the Belleville clutch were continued by the author and Mr. George Campbell, on their respective problems.

## Detailed Results

The physical problem being analyzed is illustrated in Figure 11. It is an S-shaped frame structure with rectangular 3 inch by 2 inch by .125 inch wall thickness, made of mild steel (A36) having a guaranteed minimum yield stress of 36,000 psi. The structure has two geometric planes of symmetry. The lower end of each frame member is always fully constrained and the upper end, at the barrier face, is fully constrained in some analyses and is allowed some freedom to slip, parallel to the barrier face, in other analyses. Due to the added symmetry of loading and boundary conditions,

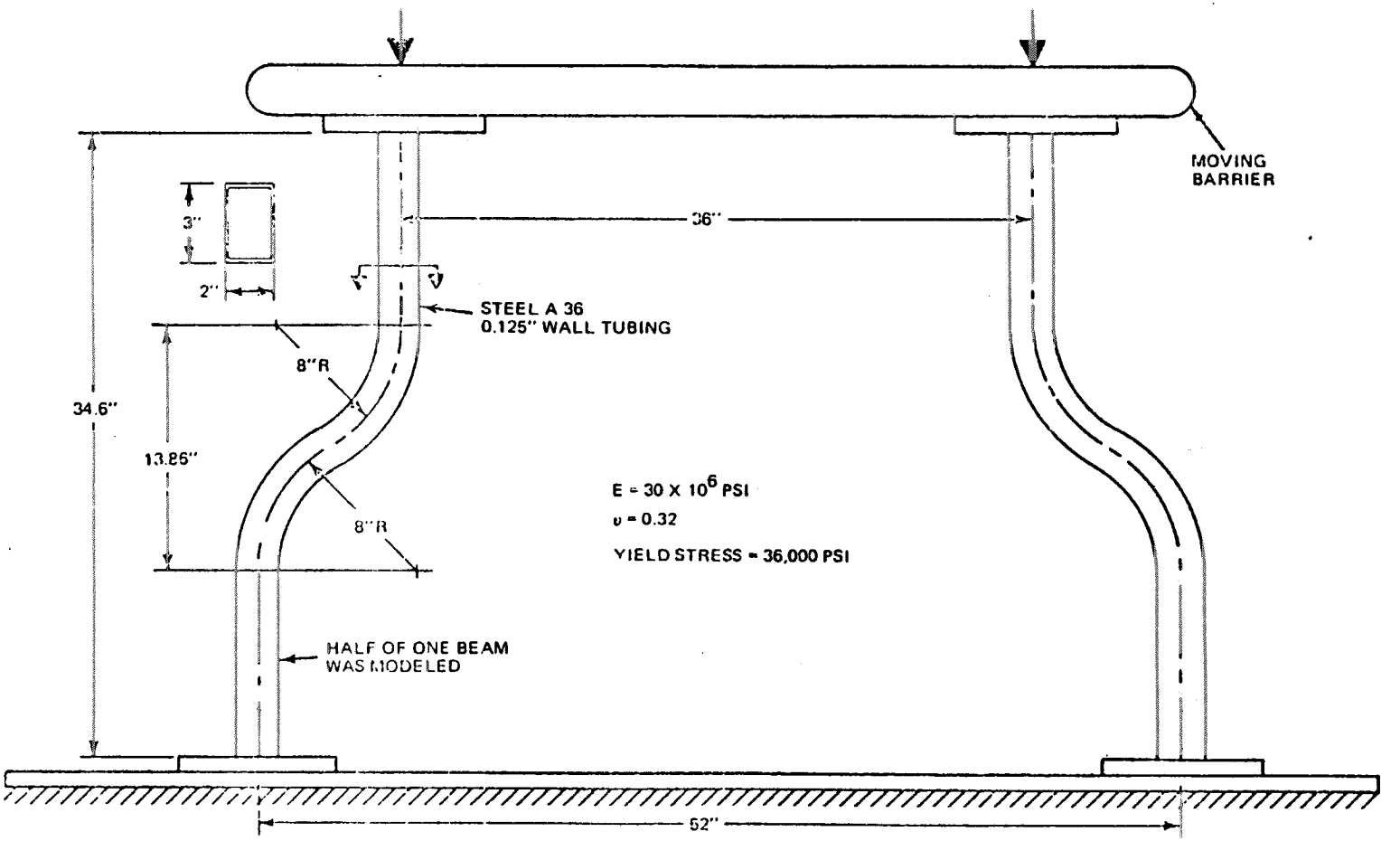


Figure 11 - S-Frame crush problem description.

an additional symmetry condition can be assumed at the inflection point between the two 8-inch radii forming the S-bend. This was done in some of the analyses so that only 1/8 of the total structure had to be modeled and analyzed.

Figure 12 shows the graphical results published in Reference #1. In this report, the analysis model results will always be compared to these test results, even though the author had limited access to and knowledge of the test procedures and final performance measures.

Figures 13 and 14 illustrate the model and predicted results as analyzed by Dr. Heng Yee Chen, BEPE. Note that the MSC/NASTRAN model predicts a barrier force curve that never decreases for increasing crush distance, up to 1 inch. The consensus at the Ford NASTRAN Users' Group Meeting, when these results were presented in November, 1981, was that this predicted poor performance correlation was due to the single point constraints (SPC's) applied to remove normal-to-the-element surface singularities.

MSC personnel remodeled the structure; the "new" model is shown in Figure 15. The model now contains 84 CQUAD4 elements, 105 Grid points, and 28 CBEAM elements. The beam elements were added to the model where plate elements come together at a character line; the adjacent elements are 90° to one another. The purpose of these added CBEAM elements is to transfer the in-plane bending loads of one plate into shear loads at the grid points for the adjacent element. If these beams are not used, the in-plane bending of one surface element is in the singular direction of the adjacent element and thus will not transfer the in-plane bending to the other surface. There was some question of how these beams affected overall results, and this was studied in one of the parameter studies that will be reviewed later.

Singularities were handled in this new model by two differing approaches: the first approach was that, in areas of the model where there was assumed to be little local deformation of the surface, single point constraints (SPC's) were used to remove the singular degrees of freedom. This was identical to the approach used initially by Dr. Heng Yee Chen.

However, during each analysis, a close check was made to assure that these SPC's were not generating significant constraint forces, by always requesting full SPC force printout and reviewing this output. If any SPC's were generating significant forces, the SPC's would have been removed and those degrees of freedom would be handled by the second approach (note that the initial selection of degrees of freedom to be handled by this method was very good - during all the analyses; the SPC-ed degrees of freedom never generated significant forces of constraint.

The second approach, to remove singularities, was that - in areas of the model where the local surface was assumed to undergo significant local deformation - "weak" torsional spring elements (CELAS) were added to the model, normal to the plate surface at one end and grounded at the other end. The torsional spring constant was selected so that the springs did not generate any large constraint forces during the simulated crush. Just as with the SPC's, the spring forces were always requested as part of the output, and were closely watched. One of the studies completed was to see how a variation of torsional stiffnesses on the CELAS elements

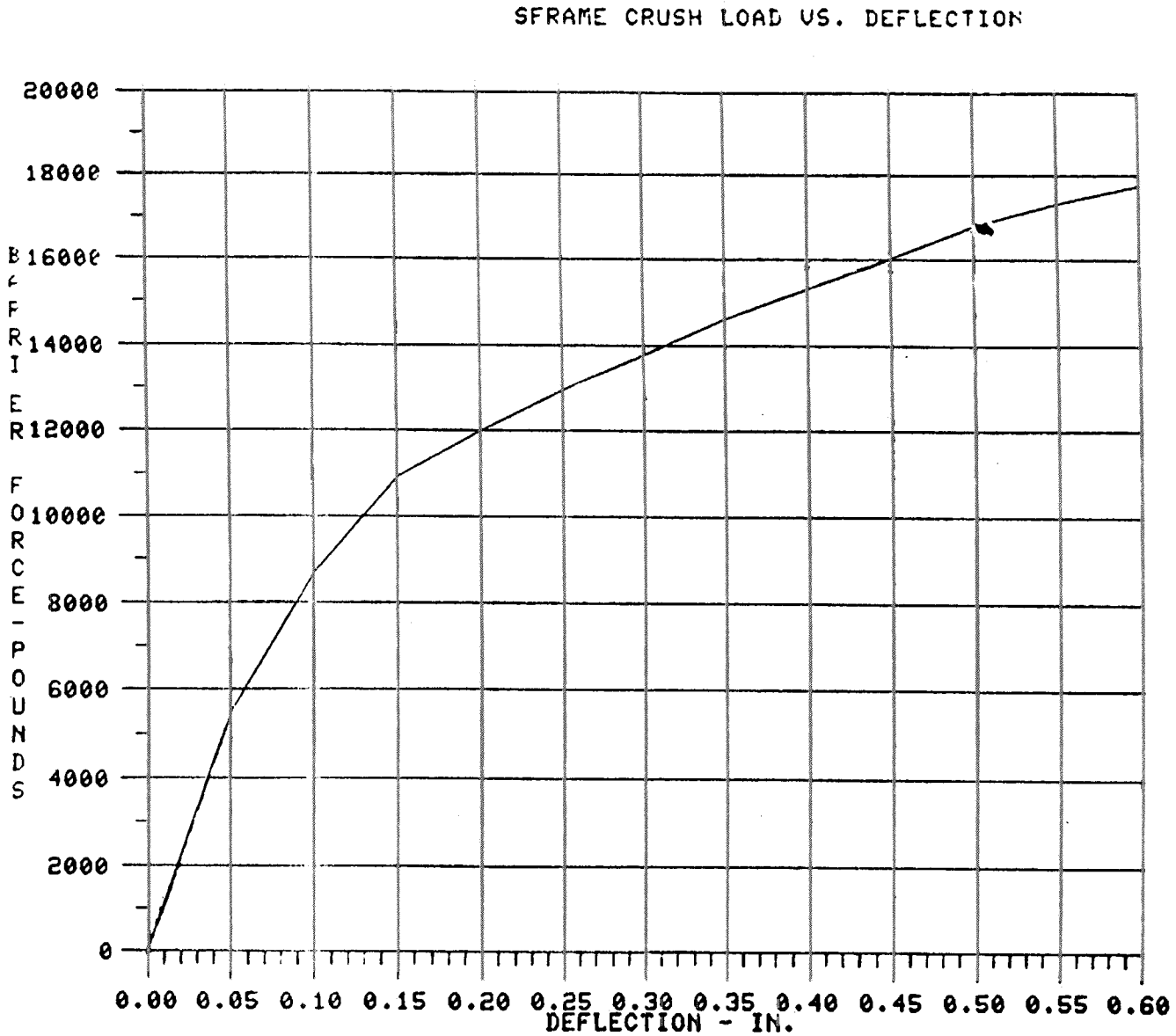


Figure 12 - Published test results.

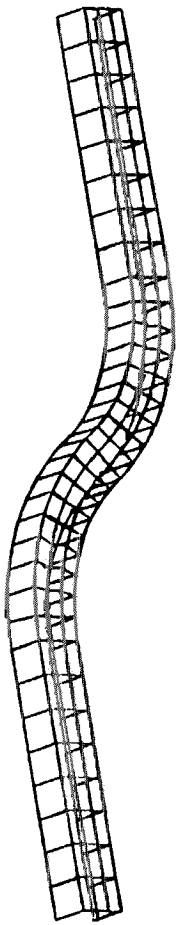

Figure 13 - BEPE 1/4 MSC/NASTRAN finite element model.

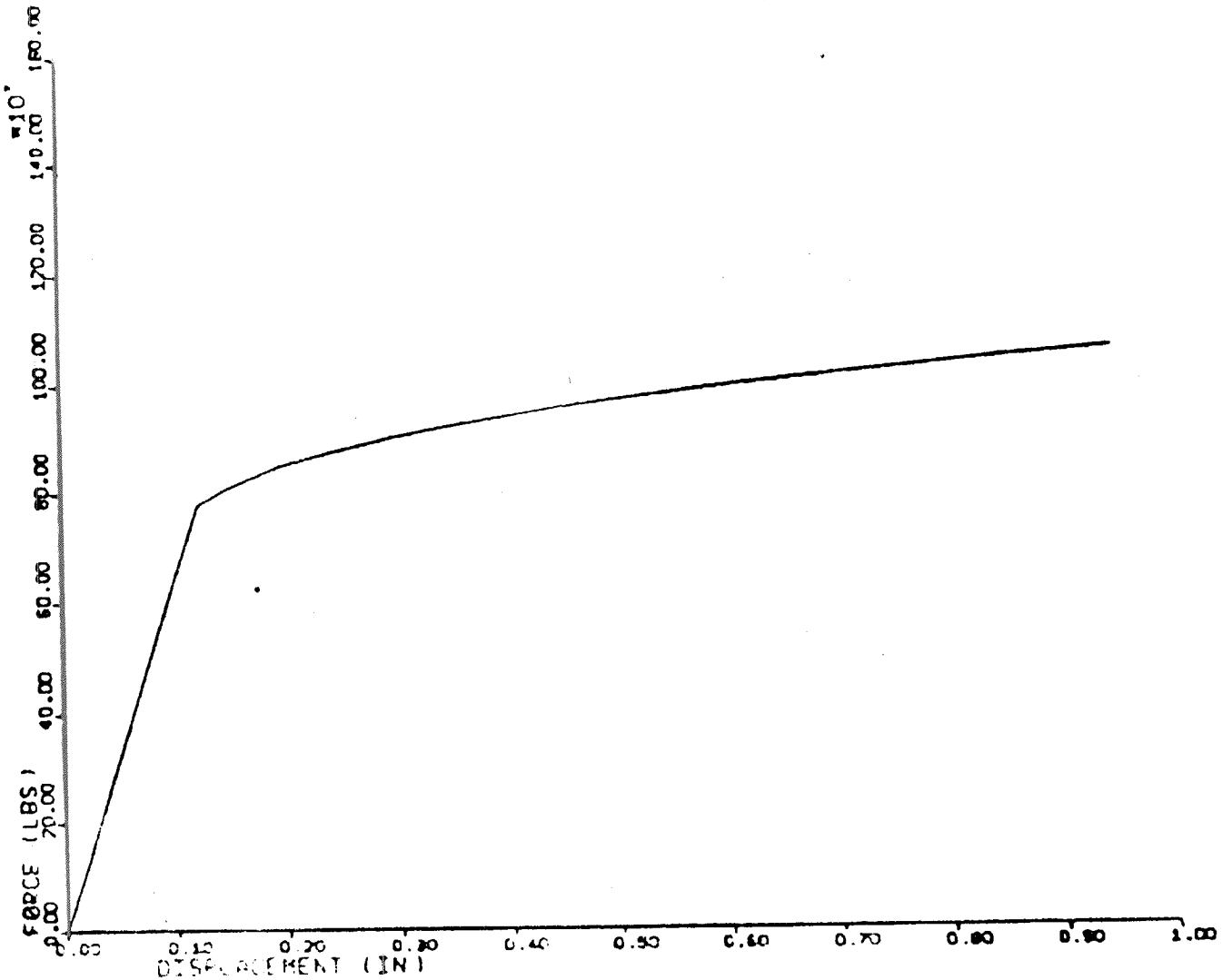


Figure 14. REBE Barrier Forces versus Crush Distance Analysis Results

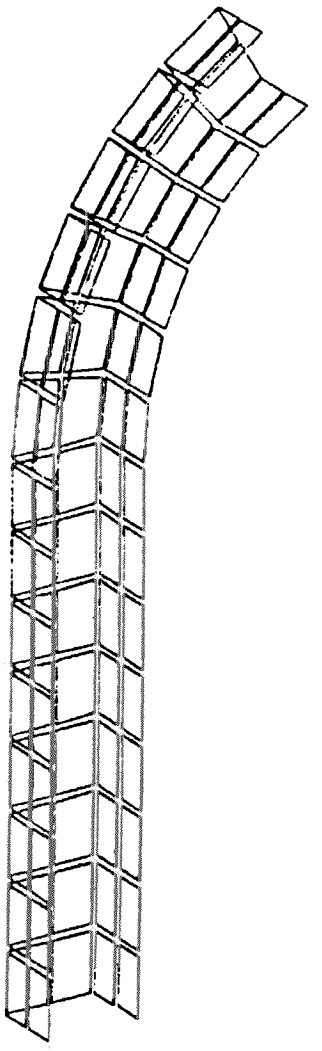

Figure 15 - Baseline finite element model (1/8 of entire structure).

affected the overall results. The conclusion was that the overall results were somewhat insensitive to the selected stiffness value for the CELAS's. A mean value for the "insensitive" region was chosen; the value was 1000 inch-pounds per radian. (The results of this parameter study will not be discussed in any more detail.)

The handling of the extra plane of symmetry at the inflection point of the S-bend was unique, and will be reviewed in detail. Figure 16 identifies the grid point numbers along this plane of load and constraint symmetry.

Figure 17 is a listing of the multipoint constraint equations (MPC's) used to enforce the symmetric deformation pattern across the plane. Note that the degrees of freedom in this area are in local cylindrical coordinates, and that the effect of the coefficients in the MPC equations is to enforce a reversing pattern about the centerline of the tube. If the displacement at a grid point on one side of the centerline is toward the fixed end of the tube, the corresponding grid point on the other side of the centerline is forced, through the MPC, to move toward the barrier face.

Figure 18 illustrates the baseline results. Note that the initial slope of the analysis-predicted barrier-force-versus-crush-distance-curve is significantly greater than that of the published test results. Also note that the maximum value of the predicted barrier force is less than that of the test results and occurs at less crush distance than that of test. These results, along with the previously discussed modeling techniques, were reviewed by the author with the Ford NASTRAN Users' Group and the following parametric studies were formulated:

> Investigate the effect of the beam "stiffness" on overall predicted performance.
>
> Study the effect on the predicted results with variations in the assumed elastic and plastic moduli, along with yield stress changes.

Figure 19 is the predicted barrier force curve as compared with test results, when the CBEAM stiffening elements were removed. The removal of the beam stiffness had negligible effect on the results. However, it was conceded that, for some analyses, it may be necessary to include them, so that local bending of one plane may be transferred as shears on the adjacent plane normal to the original surface. MSC had stated that they had reviewed a dynamic analysis for a customer where this load transfer governed the modal predictions. Since the beam elements caused no harm in this analysis, they were to be included in all subsequent analyses.

Figure 20 illustrates the predicted barrier force curves when the assumed materials are varied by 10%. Note that a 10% variation of physical properties is very slight, especially for the assumed yield stress. For A36 mild steel material, it is the author's experience that the yield stress can approach or exceed 50,000 psi on coupons made from incoming steel. Remember that the 36,000 psi value is a guaranteed minimum and that the entire population of plus or minus three standard deviations from the mean value must lie above the value of 36,000 psi.

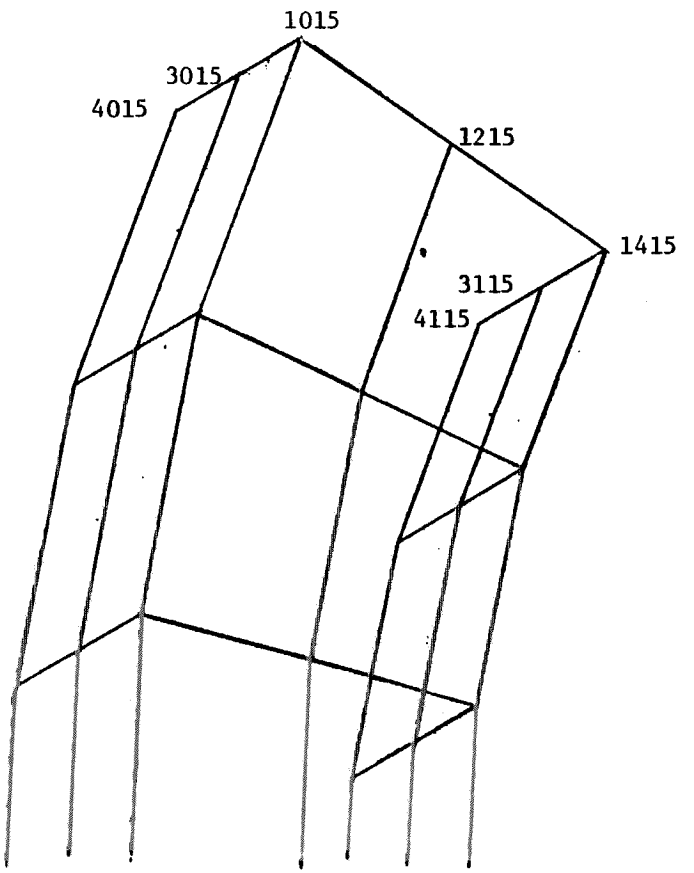


Figure 16 - Grid point numbers at plane of symmetry.

```
MPC.50.4015.1.1.0.4115.1.1.0
MPC.50.4015.2.1.0.4115.2.1.0
MPC.50.3015.1.1.0.3115.1.1.0
MPC.50.3015.2.1.0.3115.2.1.0
MPC.50.3015.4.1.0.3115.4.1.0
MPC.50.3015.5.1.0.3115.5.1.0
MPC.50.1015.1.1.0.1415.1.1.0
MPC.50.1015.2.1.0.1415.2.1.0
MPC.50.1015.4.1.0.1415.4.1.0
MPC.50.1015.5.1.0.1415.5.1.0
```

Figure 17 - Multipoint constraint equations for symmetry.

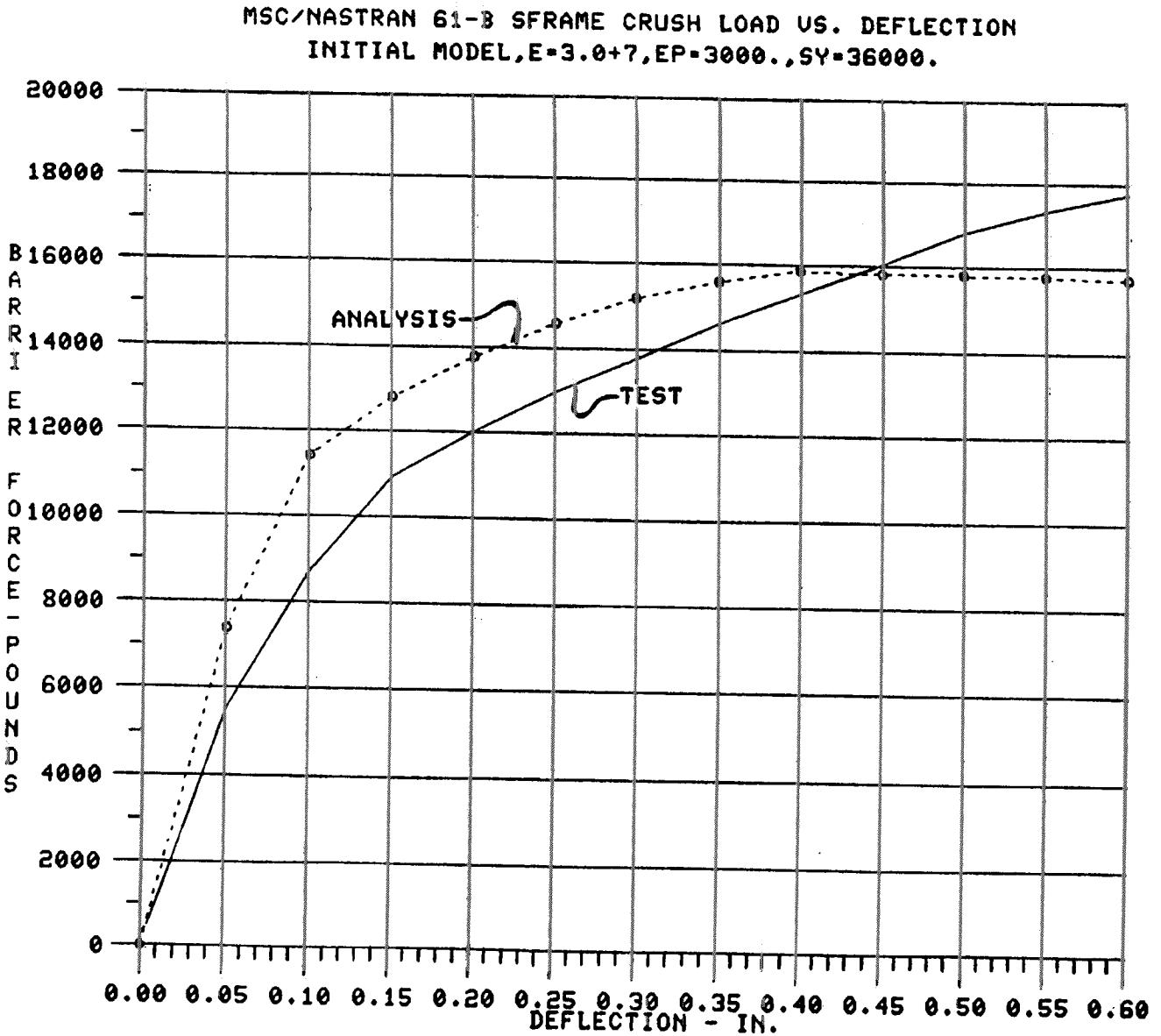


Figure 18 - Baseline analysis results versus published test results.

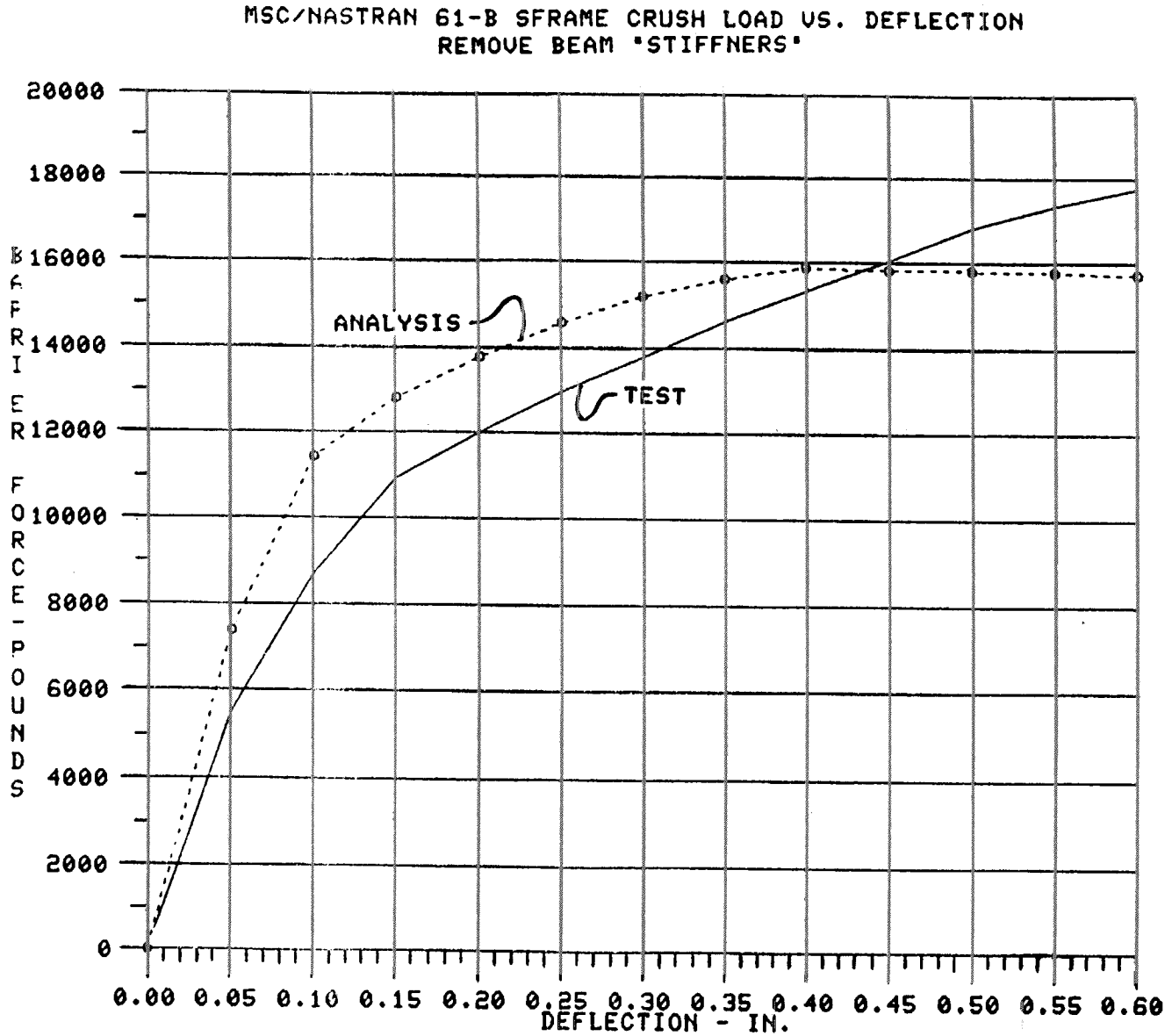


Figure 19 - Analytically-predicted barrier force versus crush distance with "CBEAMS" removed.

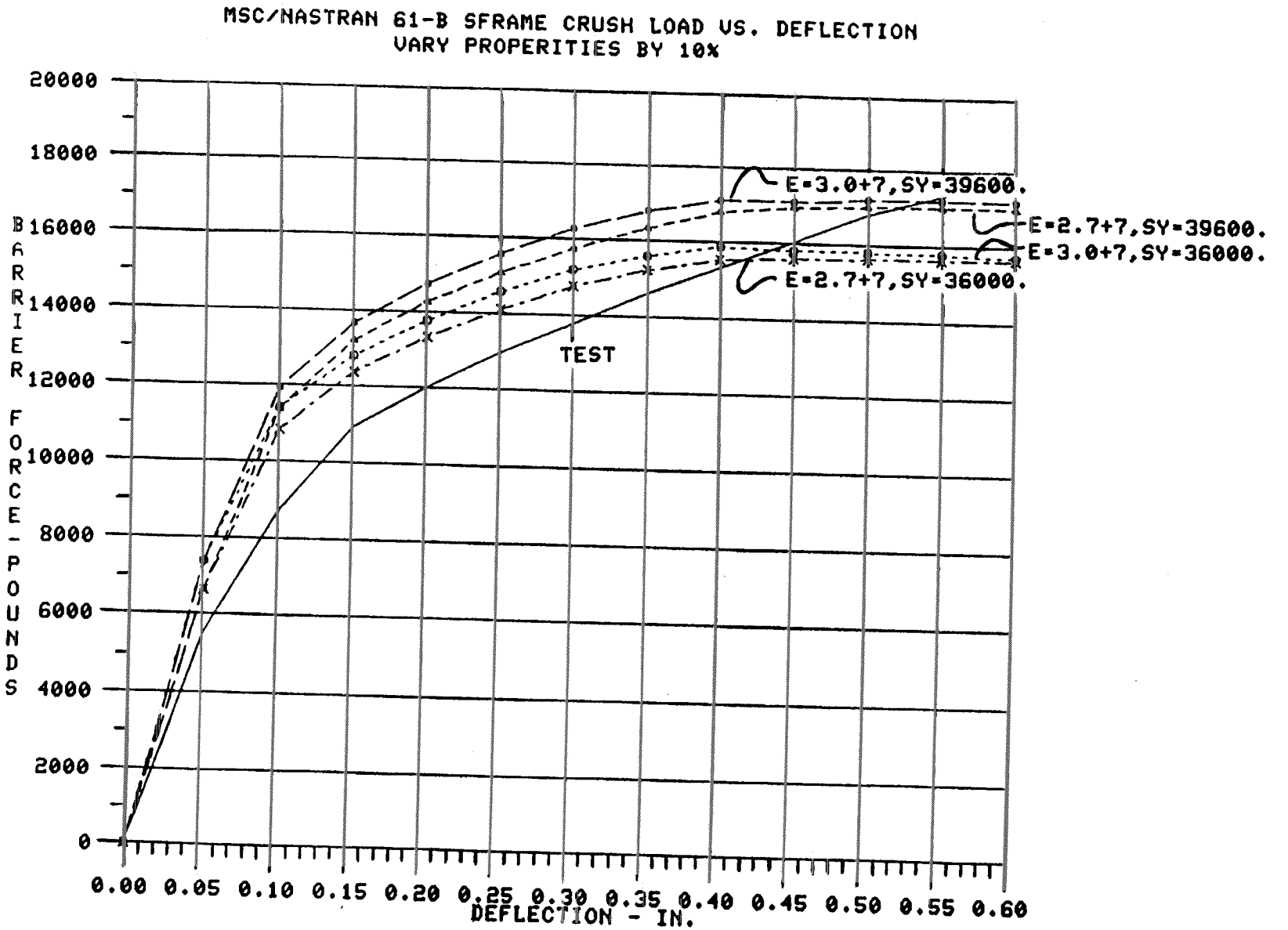


Figure 20 - Decrease elastic modulus 10%, increase yield stress 10%.

Figure 20 shows that the initial slope of the curve is sensitive to the assumed elastic modulus (the curves where the two elastic moduli values are 30 million psi lie on top of one another; the same is true when the assumed elastic modulus is 27 million psi) and that the maximum barrier force and crush distance where the maximum force is reached is sensitive to the assumed yield stress (the pairs of curves, one pair for 36,000 psi and one pair for 39,600 psi, almost fall upon one another). The two effects, initial slope and maximum barrier force generated, are almost uncoupled from one another. This suggests that, if the initial slope is incorrect, an educated adjustment of the elastic modulus can be made. If the maximum barrier force and associated crush distance at maximum force is incorrect, an adjustment of the yield stress can be used.

Figure 21 shows further adjustment of the assumed material properties. In this figure, the elastic modulus was reduced 20% from the original value (24 million psi versus 30 million psi) and the yield stress is increased 15% (41,400 psi versus 36,000 psi). Note that now the initial slope and the maximum barrier force compares favorably with that of test results. However, the crush distance where the maximum barrier force is developed is in error ( .5 inch for analysis - .6 inch for test). Also, the slopes of the curves in the mid-range for crush distance are significantly different. If energy absorption is a major criteria, even though the initial slopes and maximum developed forces correlate, the total energy absorbed is significantly different between analysis and test results.

Further material property variations were studied. The impetus for these further investigations was the published results for the same problem using WRECKER/FORD (Reference #3), a Ford-developed in-house program for non-linear analysis. In the WRECKER/FORD documentation, a curve is published (Figure 22) showing how the barrier force curves for this S-Frame problem are affected by large variations in assumed plastic modulus.

Figure 23 shows the effects in MSC/NASTRAN with small changes in plastic modulus. All analyses conducted up to this point used an assumed plastic modulus that was one-ten-thousandth of the assumed elastic modulus. With plastic moduli of 0, 1/100,000, 1/10,000 and 1/1000 of the elastic modulus, the results are almost identical. However, this problem with a non-zero plastic modulus is mathematically better behaved than one with a zero plastic modulus. It converged to the solution with less iterations and with less computer time than that with a zero plastic modulus.

Figures 24 and 25 show the results with large plastic modulus values, comparable to the WRECKER/FORD curves. With plastic modulus values equal to or greater than $4.9 \times 10^4$, there is never a clear "maximum" barrier force; ie, the curves are constantly increasing.

As before, these new results were presented to the Ford NASTRAN Users' Group, and there was considerable discussion as to why the initial slope of the barrier force versus crush distance curve was so far off from that of test. Two potential problem areas were suggested: first, the model is somewhat coarse; second, the boundary conditions may not match that of the test (this difficulty would have been resolved if the testing was completed in-house). It was suggested that the model was too coarse (see Figure 26), in areas where excessive deformation was taking place.

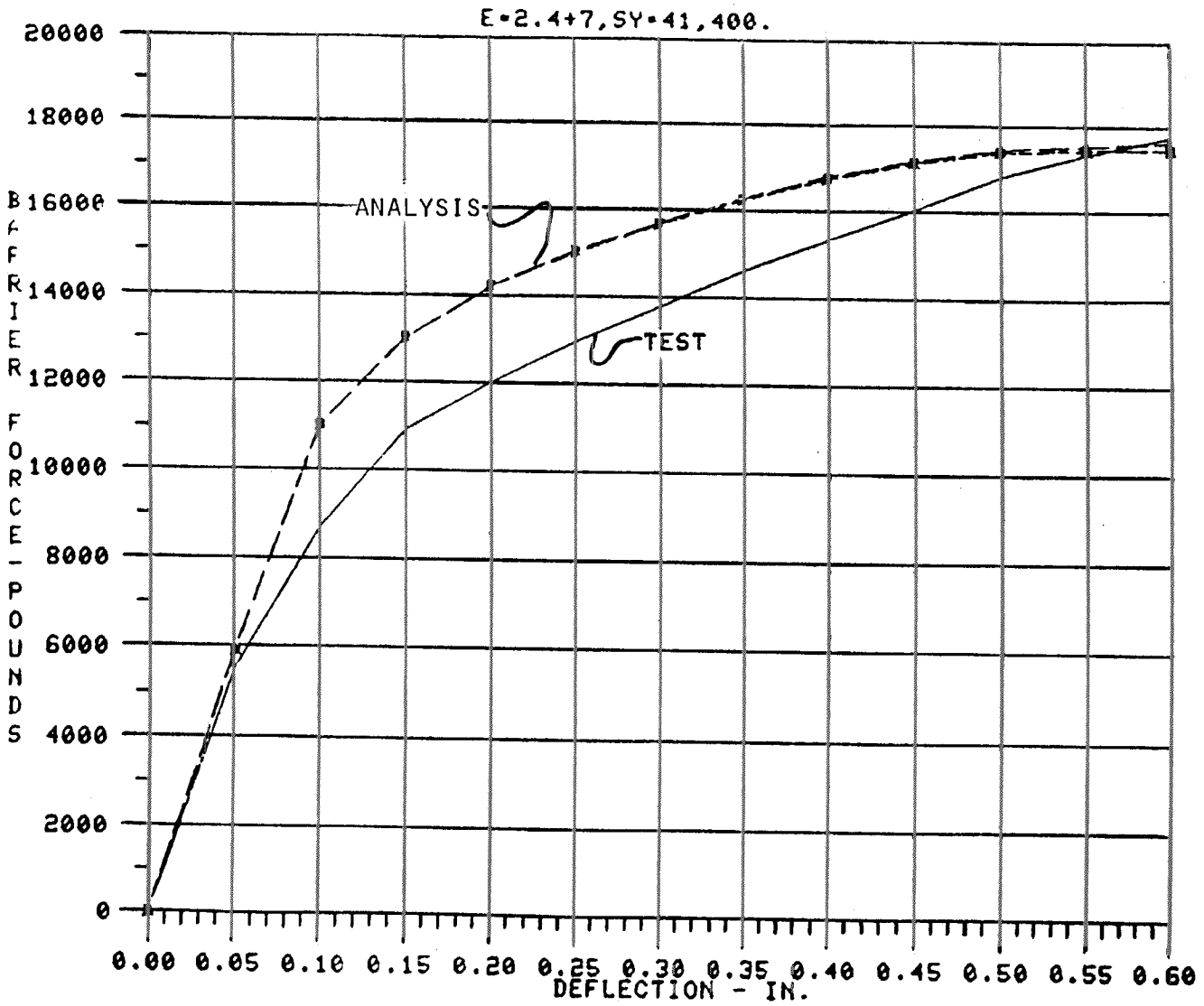


Figure 21 - Decrease elastic modulus 20%, increase yield stress 15%.

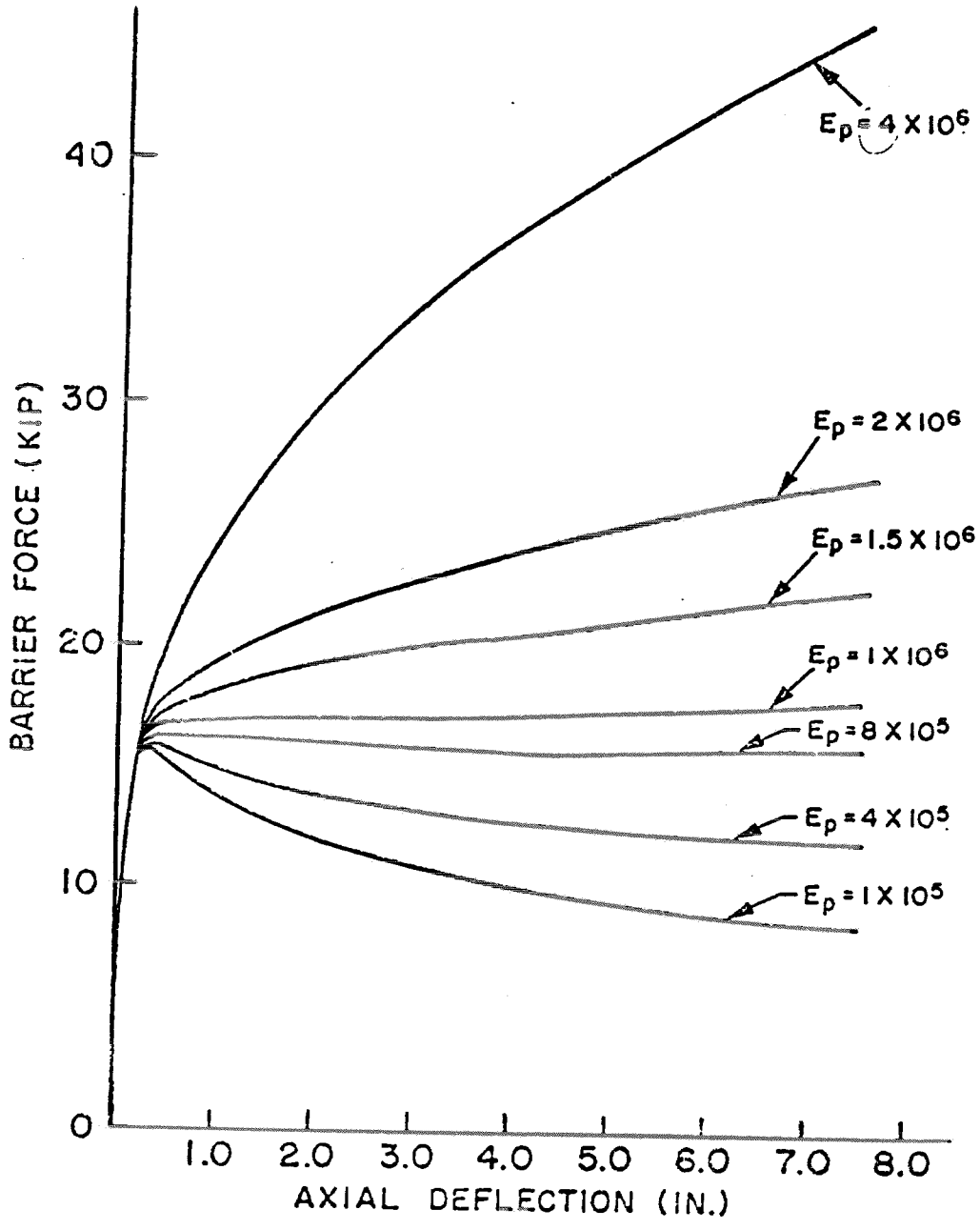


Figure 22 - WRECKER/FORD S-Frame curves with a varying plastic modulus, Ep

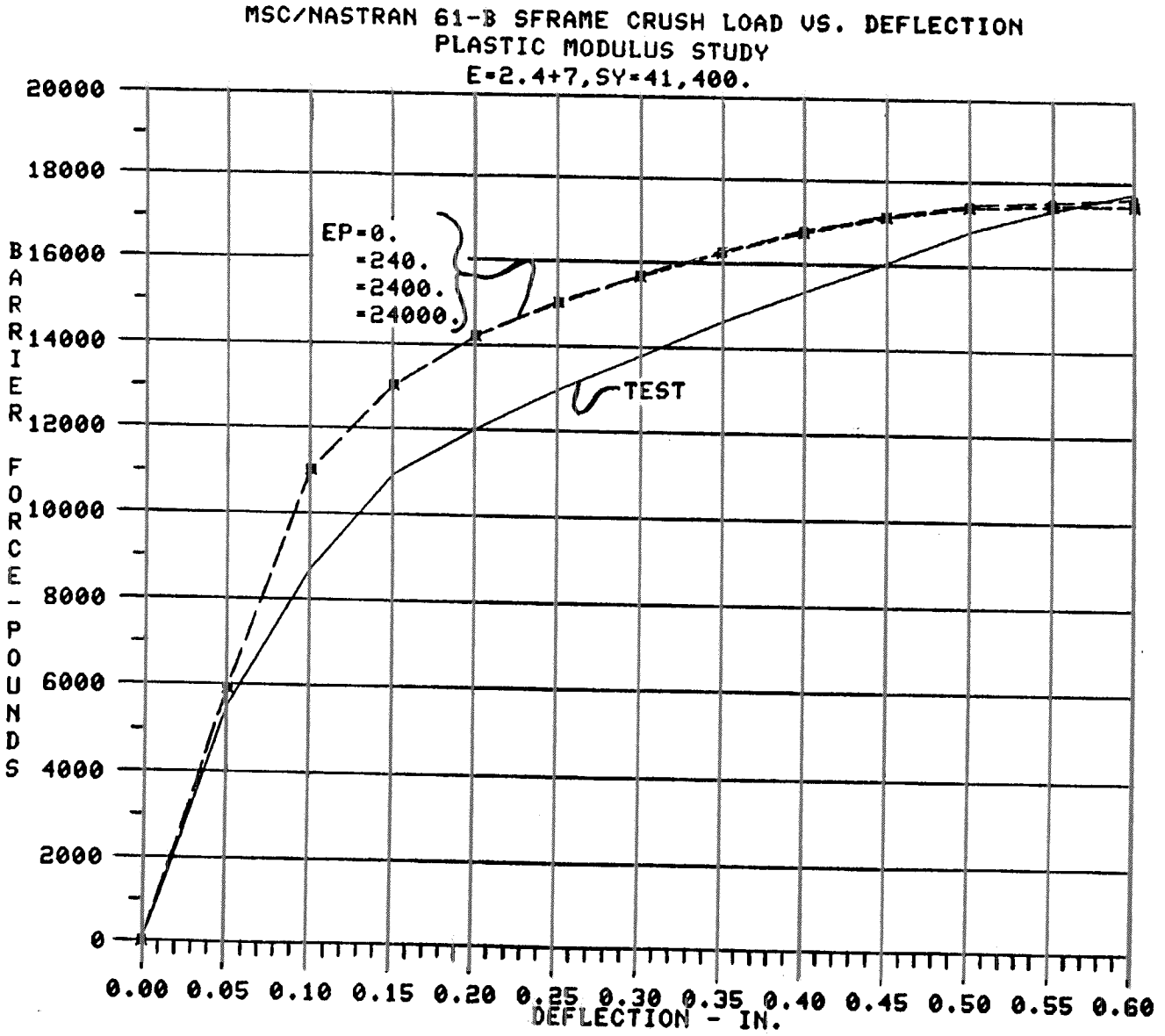


Figure 23 - Barrier force curves with varying small values of plastic modulus.

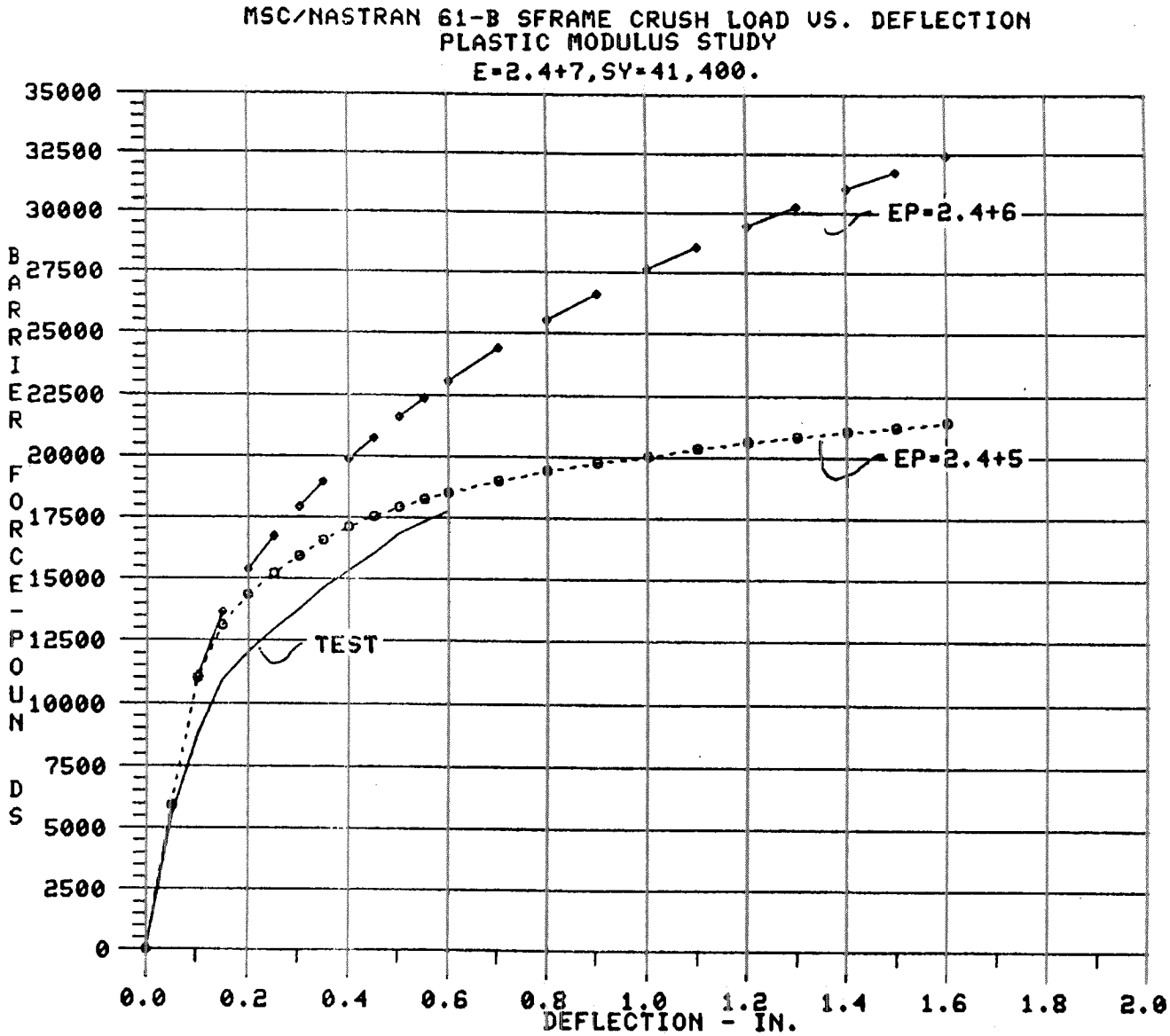


Figure 24 - Barrier force curves with varying large values of plastic modulus.

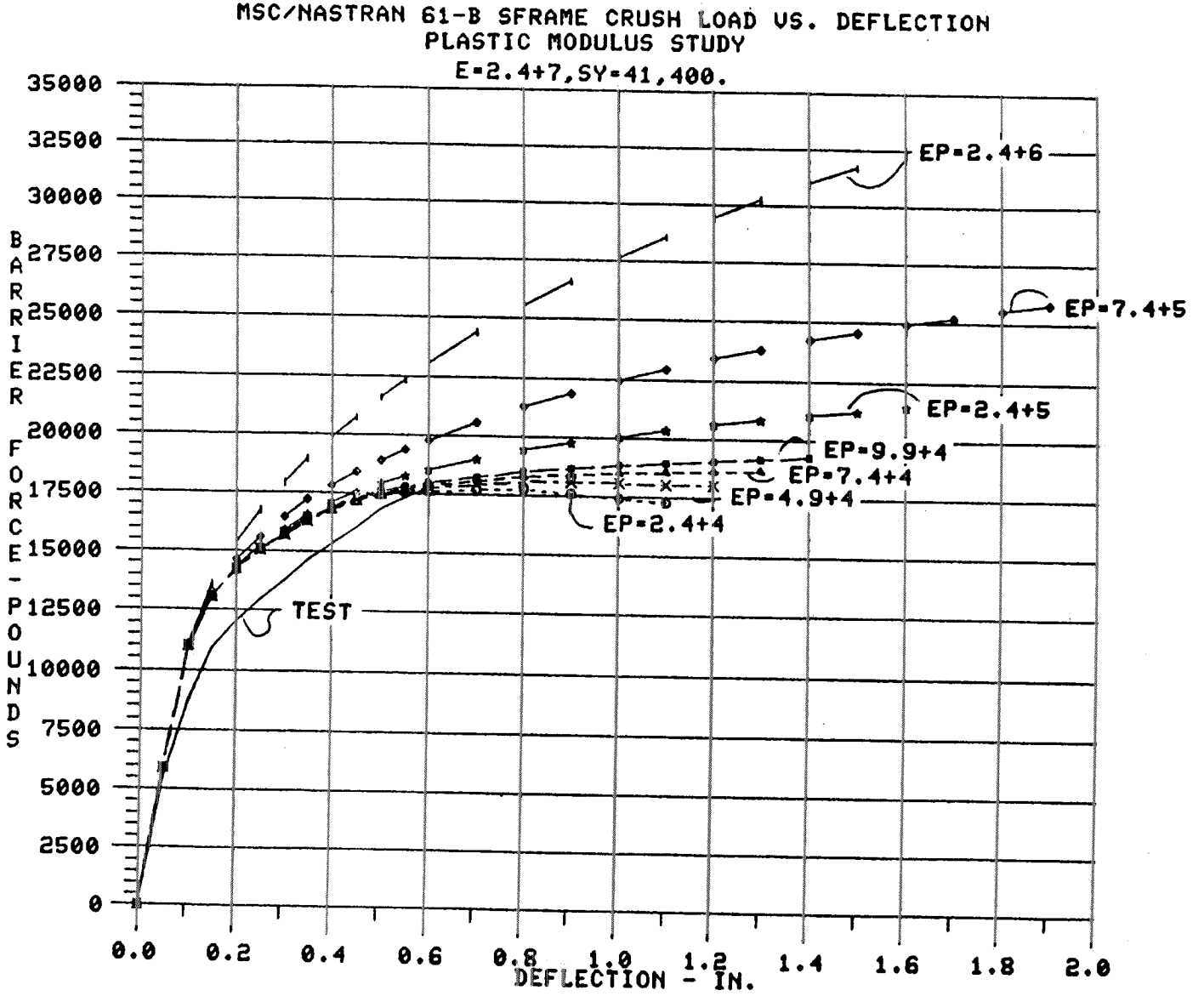


Figure 25 - Barrier force curves with varying large values of plastic modulus.

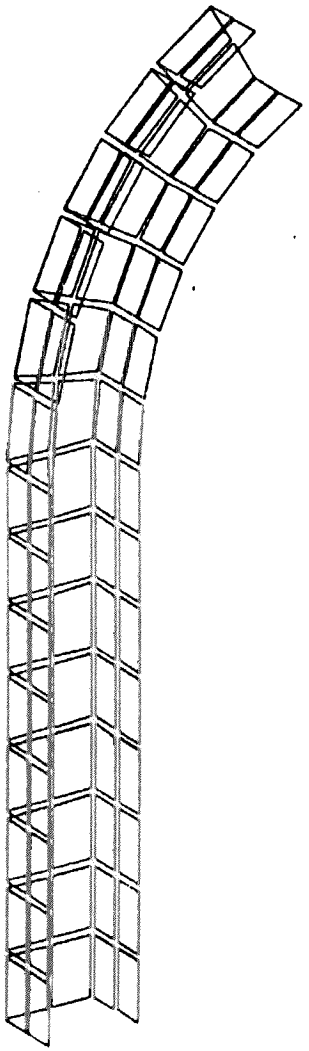

Figure 26 - Baseline "coarse" finite element model.

A new model was created (Figure 27) having much more detail at the curved areas. Figure 28 shows the results from this new model compared with the baseline model and test results. The new model was created in the hope that the initial slope correlation problem would be resolved. It was not. Not only that, but the new model was much more costly to execute, was numerically more unstable and, with the onset of local deformation, the model yielded much too quickly. Like the time before with the baseline model, the approach was now to drop the assumed elastic modulus and increase the assumed yield stress (elastic modulus dropped from 30 million psi to 24 million psi; the yield stress increased from 36,000 psi to 41,400 psi - see Figure 29). The correlation to the test results was much better, but the model was too costly to run, so this more detailed modeling approach was dropped.

At this point in the series of analyses, the boundary conditions came into question. Perhaps the test fixturing allowed some side slip at the barrier face. For example, for vehicle certification tests, the barrier surface is covered with plywood, perhaps allowing the structure to slide laterally. Also, reference #2 notes -

> "....this problem was extremely sensitive to any boundary condition modification. Due to limited access to the experimental results, test simulation was initially difficult".

The author expressed our sentiments exactly!

A meeting was held with BEPE personnel to review the analysis results obtained up to this point. A non-linear 1/4 model of the S-frame was analyzed by their engineers, using a competitive program (ANSYS, a product of Swanson Analysis Systems, Inc.). Results from the competitive program seemed to indicate that - in order to include slippage at the barrier face - a 1/4 model was necessary.

In order to establish whether a 1/4 model or a 1/8 model was necessary, a new MSC/NASTRAN model (1/4 of the entire structure - see Figure 30) was created, with the same mesh density as the original 1/8 model, but no longer assuming "symmetry" of displacements about the plane through the inflection point of the S-bend. With the boundary condition at the barrier face removed, Figure 31 shows the results from the 1/8 model, the 1/4 model and test.

Both the 1/4 model, fully constrained at the bottom end and free to move parallel to the barrier face at the upper end, and the 1/8 model, free to move parallel to the barrier face on "both" ends, produced the same results. The results from both of these models were much less than test. Since all previous models were stiffer than test and these two models were more flexible than test, the inference may be that the barrier does not allow complete, unrestrained movement at the barrier, but applies to the S-Frame a slight constraint to sideways movement.

The next series of analyses (Figures 32 and 33) demonstrate how the model responds to various barrier fixities. The 1/8 model was used, since it performs satisfactorily and is less costly than the 1/4 model. Linear spring elements (CELAS's) were added between the grid points at the simulated barrier face and ground in the direction of allowed barrier slip. Iterating on the barrier plywood face spring rate (the final value chosen was 3500 pounds per inch), and elevating the assumed yield stress to

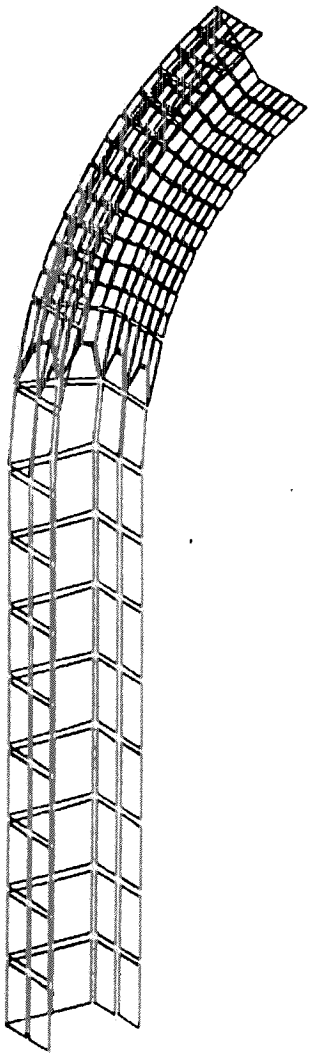

Figure 27 - New "Fine" finite element model.

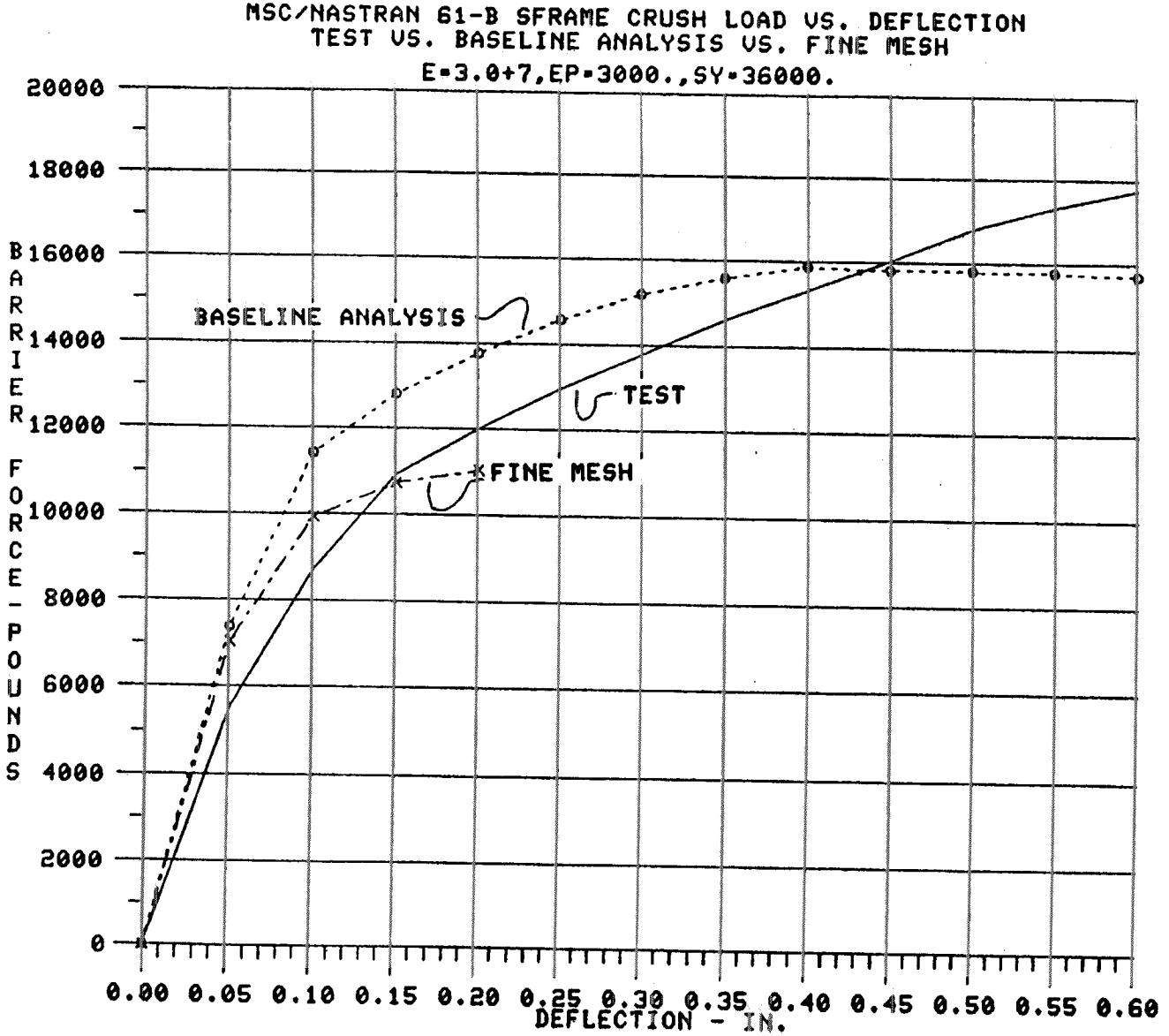


Figure 28 - New "Fine" Model Barrier Force versus Crush Distance curve with baseline material properties.

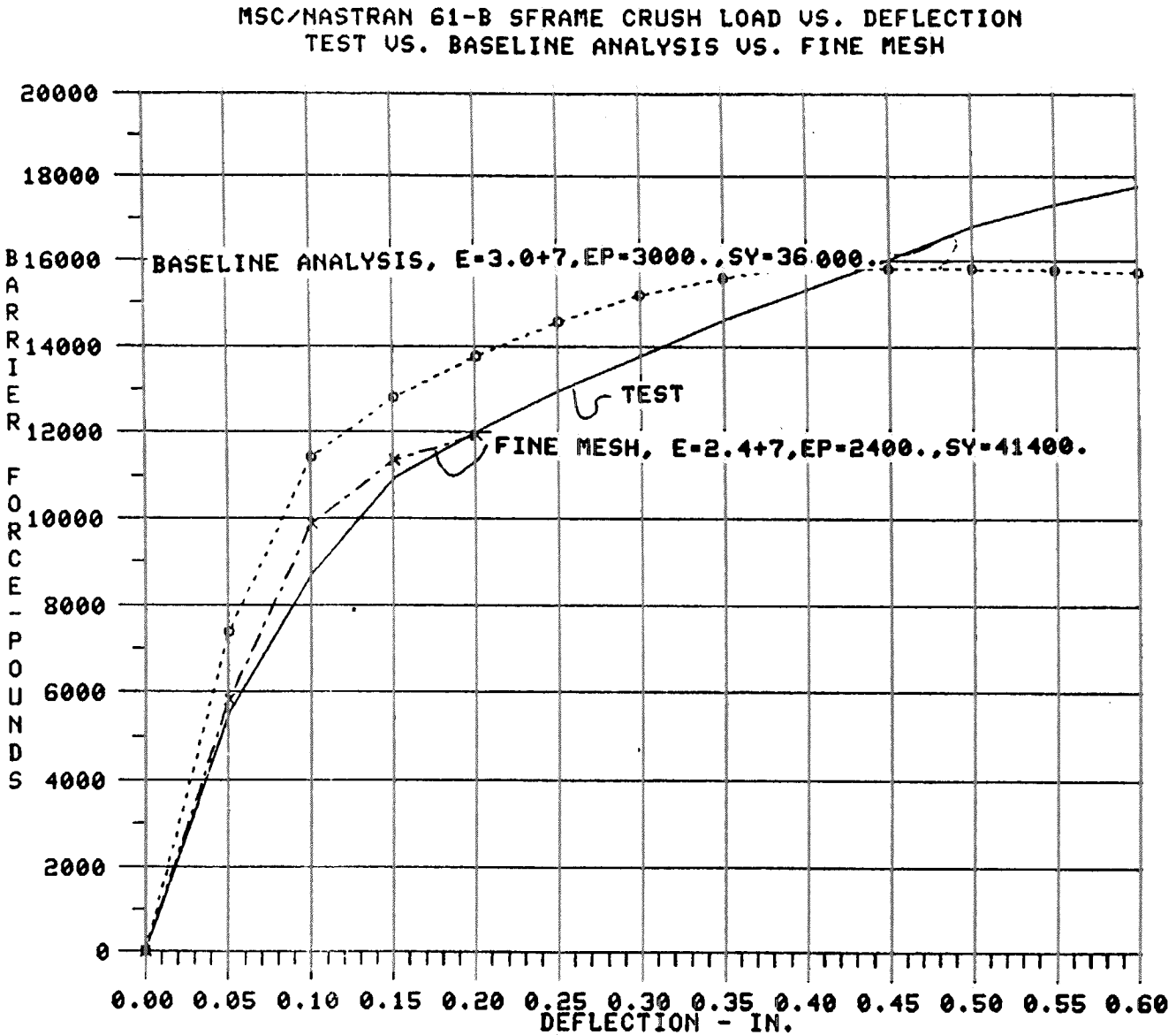


Figure 29 - New "Fine" model Barrier Force versus Crush Distance curve with revised material properties.

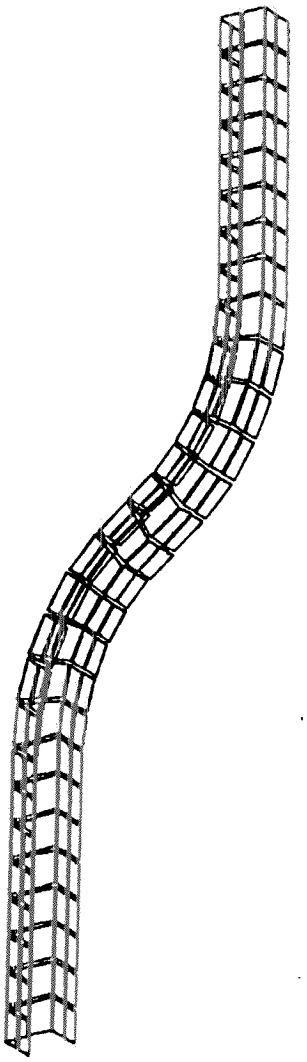

Figure 30 - 1/4 model with same mesh density as baseline 1/8 model.

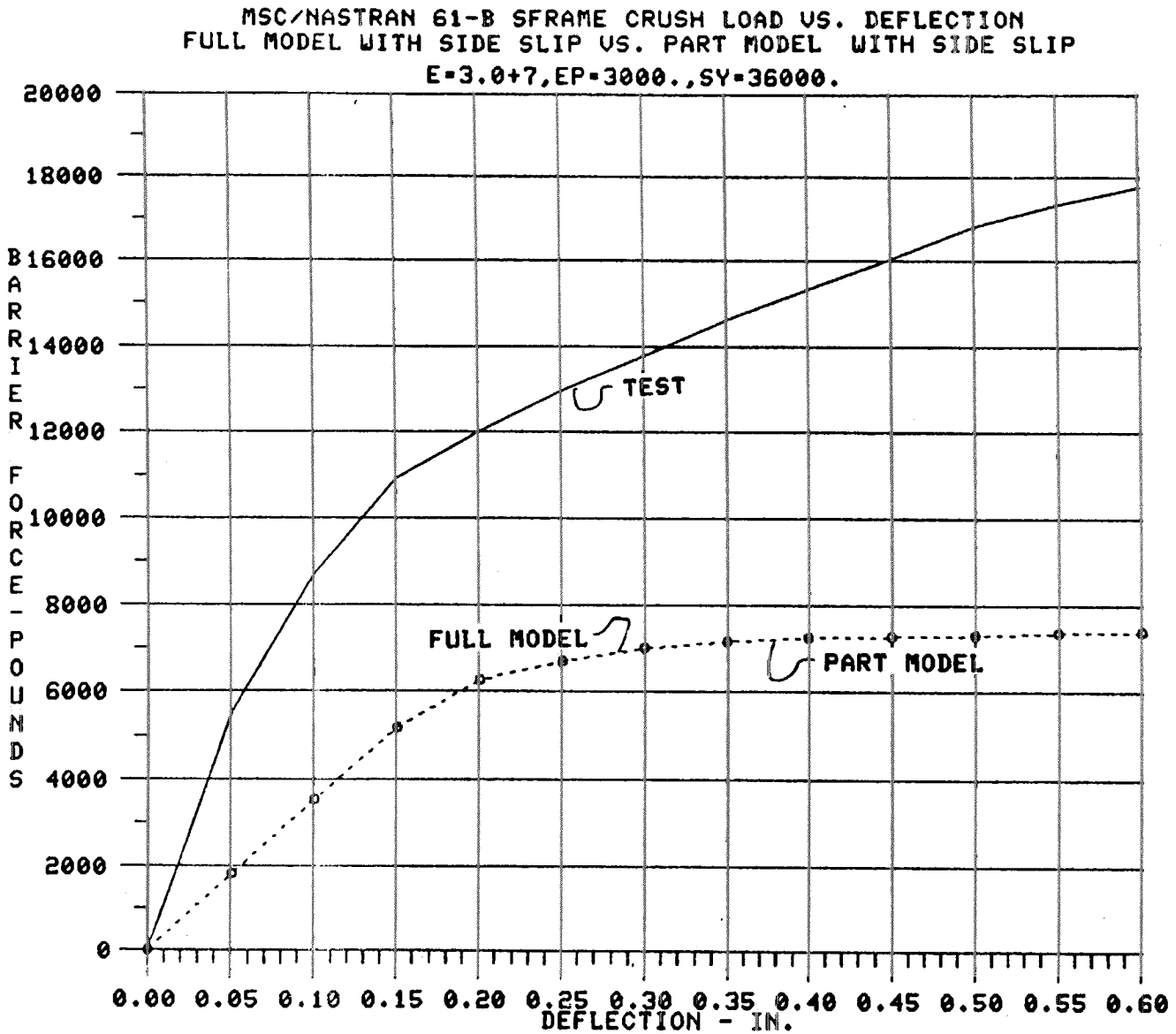


Figure 31 - 1/4 model and 1/8 model Barrier Force versus Crush Distance with slip allowed at barrier.

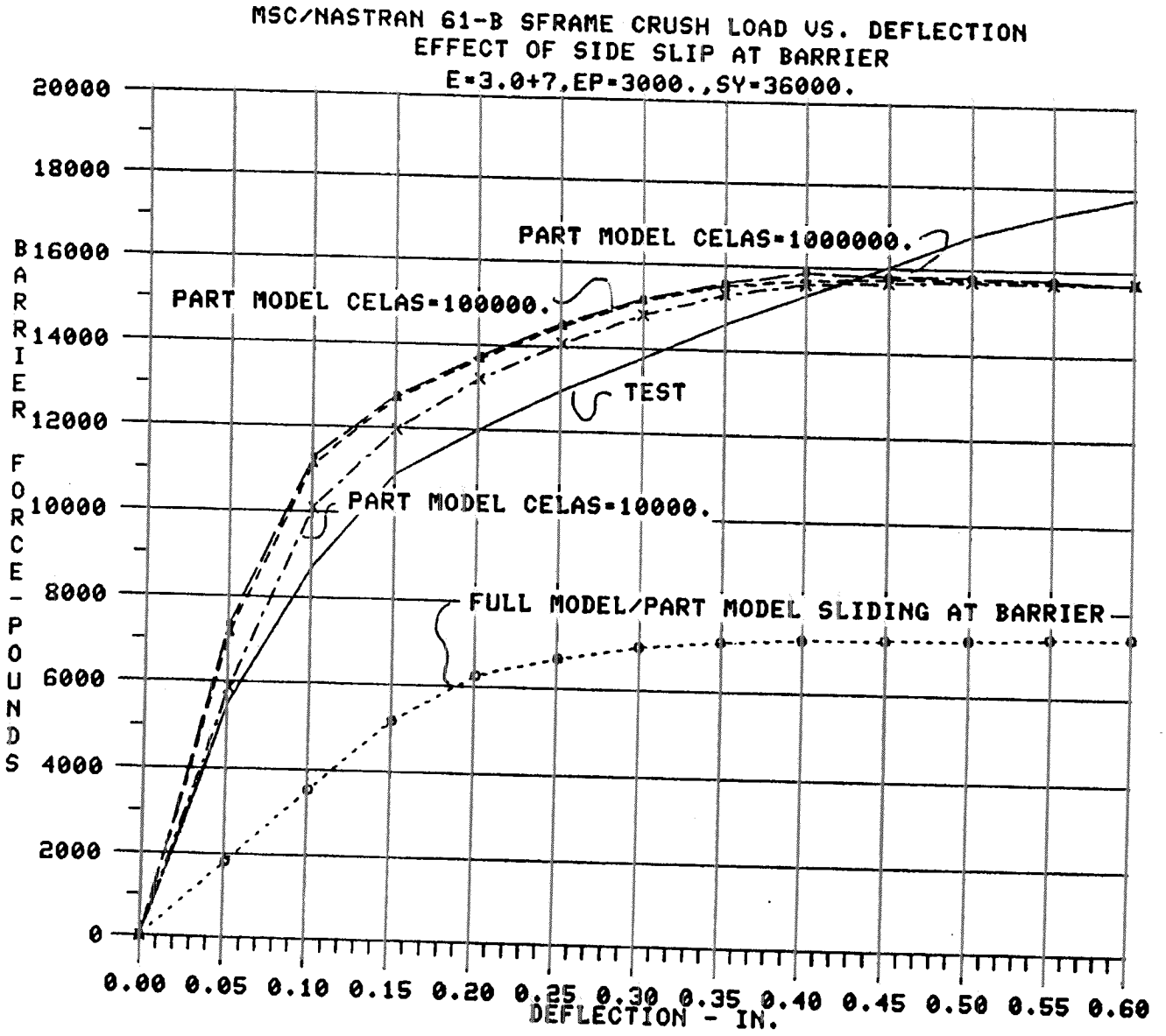


Figure 32 - Barrier Force versus Crush Distance for barrier fixities from 10,000 to 1,000,000 lbs./in. at each point.

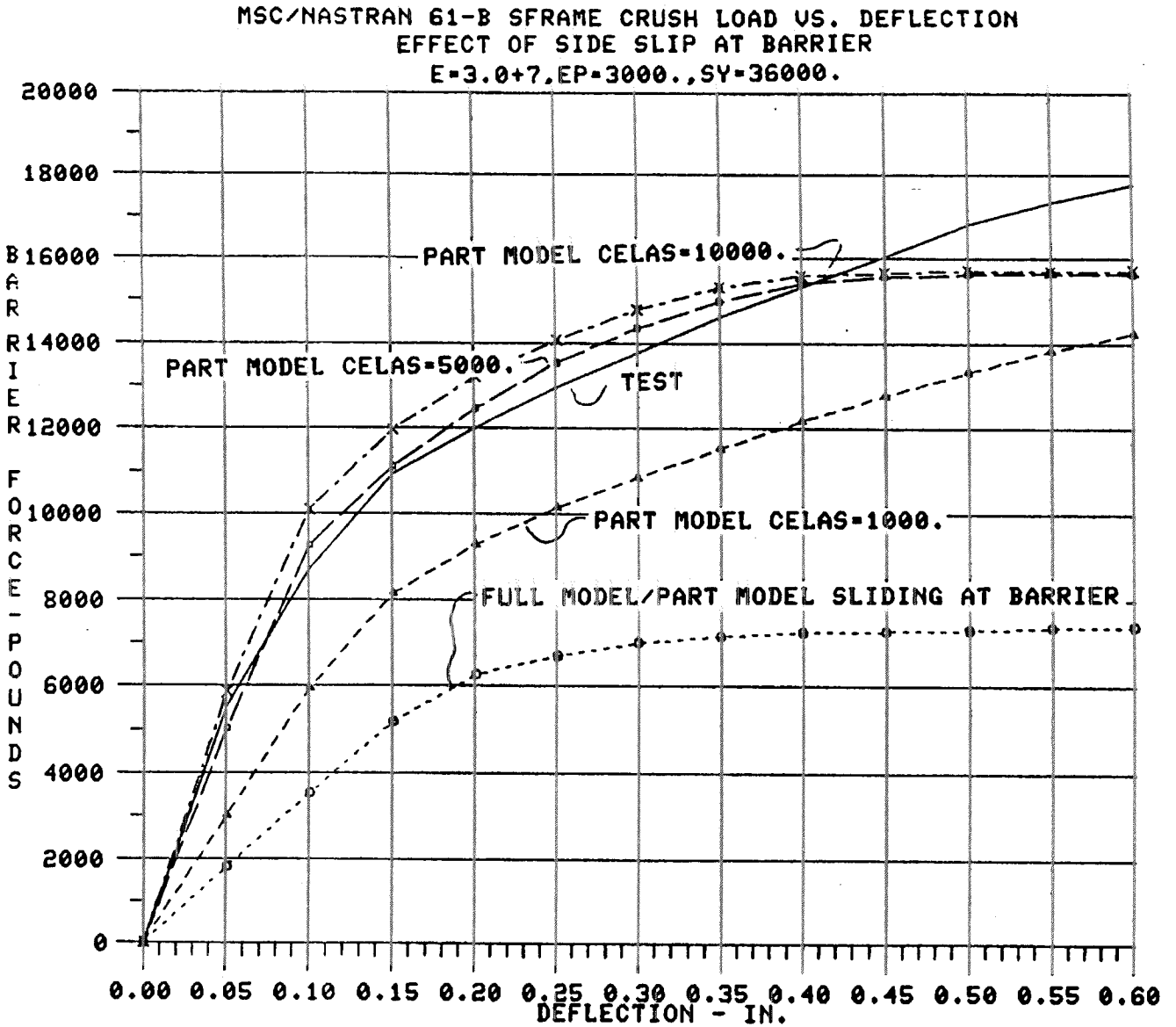


Figure 33 - Barrier Force versus Crush Distance for barrier fixities from 1,000 to 10,000 lbs./in. at each point.

41,400 psi, Figure 34 shows the "Final" correlation. The initial part of the curve brackets the test curve, the maximum barrier force is accurately predicted, and the maximum deviation between analysis and test is approximately 1200 pounds.

In summary, the conclusion can be reached that an analyst can match a test curve well enough with an analysis if he is given enough variables to iterate. The test curve was matched as long as the model is allowed to slip parallel to the barrier face, with a given amount of plywood-face spring rate, with the yield stress elevated 15% from its guaranteed minimum value. Almost any problem can be simulated, given enough variables and unlimited perseverance. This "final" conclusion is not at all satisfying!

All previous results were discussed at another Ford NASTRAN Users' Group Meeting. Throwing out most of the experience gained to this point, the meeting attendees reviewed the initial assumptions. It was concluded that the elastic-perfect plastic assumption be abandoned, and that an actual stress-strain curve be obtained and used in the analysis. Ford has a materials data base, used principally for fatigue predictions. The data base contains not only fatigue data but for 36,000 psi guaranteed yield mild steel, 3 cyclic stress-strain graphs as well (see Figures 35 thru 43). Using the baseline 1/8 model, assuming fixity at both ends of the beam, and using the three materials graphs in digitized form, Figures 44, 45 and 46 resulted. Figure 47 is a composite of these three results. Using the stress-strain data, the predicted barrier force is never more than 1000 pounds from the test results. In fact, for materials' file #78, the variance between analysis and published test results is usually less than 500 pounds for the entire range of crush distances.

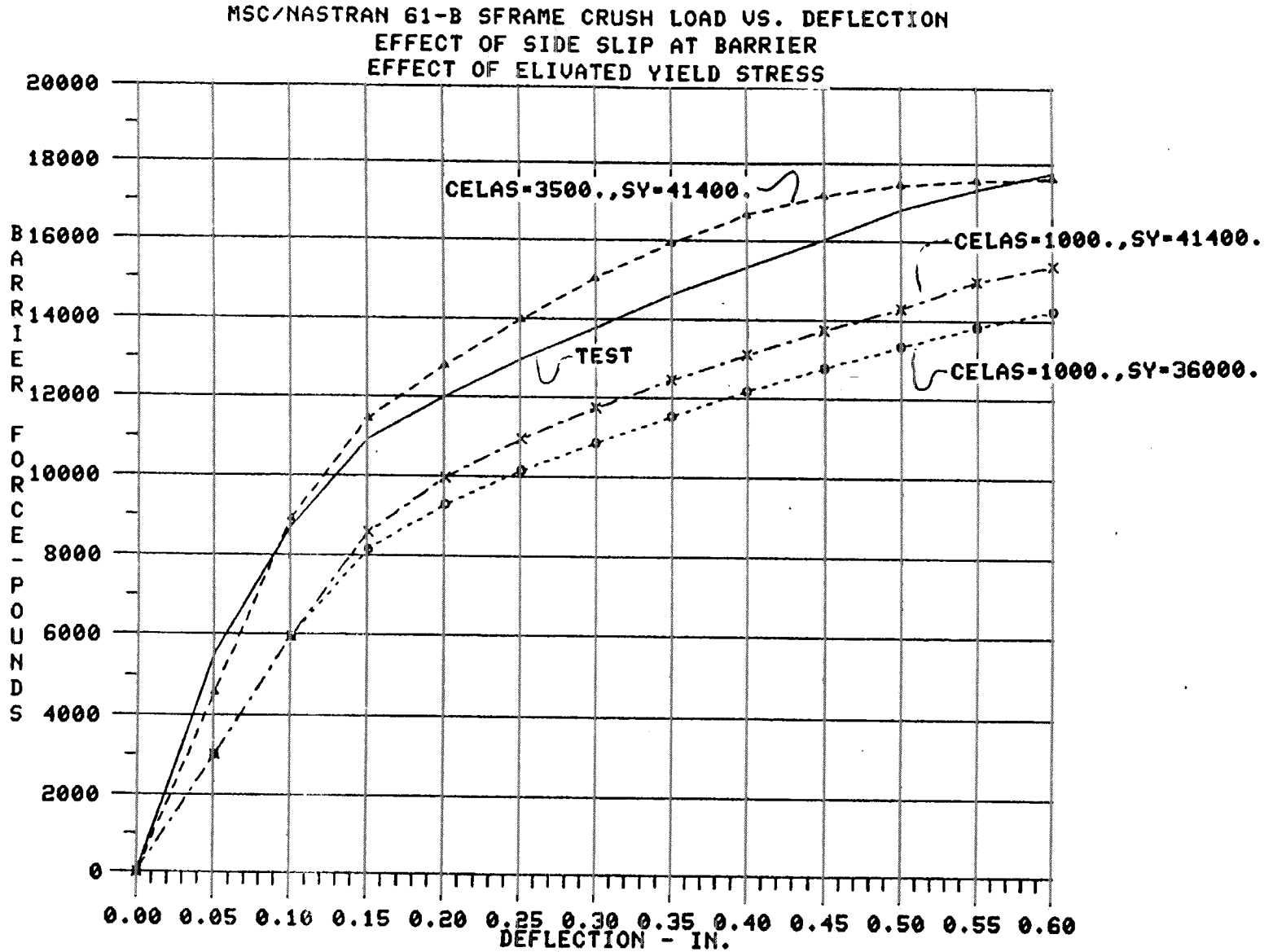


Figure 34 - Barrier Force versus Crush Distance for 2 barrier fixities (1,000 and 3,500 lbs./in.).

```
SAE1006
AISI 1006
LOW CARBON, HOT ROLLED,
PIETROWSKI,  DOFASCO,  OCT77
BHN 85



SAE1006      S1006C59     SHR     F1075
MOD = 30023.     YLD 0.2%=  36.     ULT.STR.=  46.
K=  60.     N=  .145
BHN=  85.  %RA= 73.    SF=     0.    EF= 0.00
```

Figure 35 - Physical properties - materials file number 75.

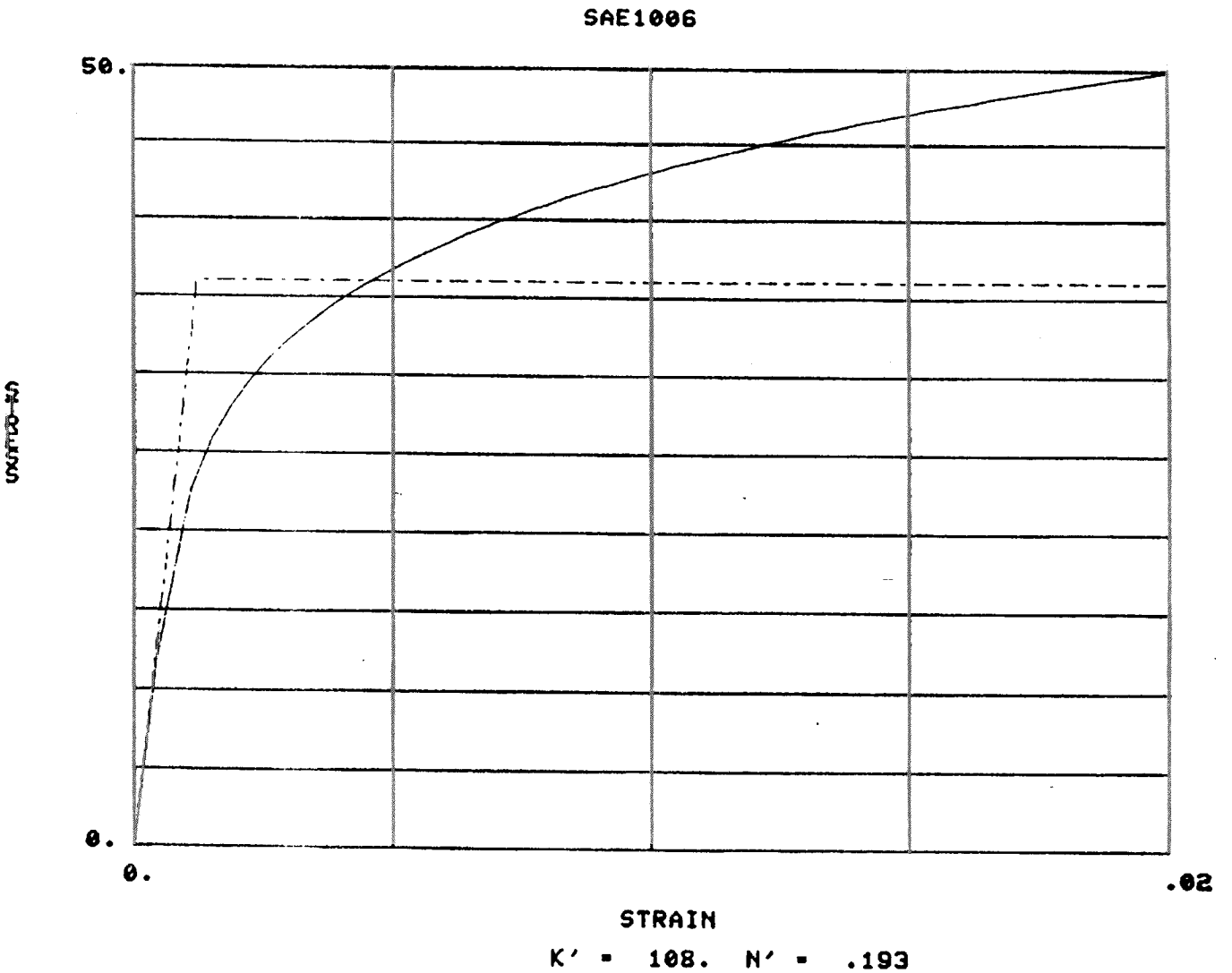


Figure 36 - Stress/Strain curve for materials file number 75.

| STRAIN | STRESS |
|---|---|
| .0 | .0 |
| .00125 | 23,440 |
| .0025 | 30,676 |
| .005 | 36,904 |
| .0075 | 40,766 |
| .01 | 43,453 |
| .0125 | 45,279 |
| .015 | 47,319 |
| .0175 | 48,820 |
| .02 | 50,000 |

DIGITIZED STRESS/STRAIN DATA - MATERIALS FILE NUMBER 75

FIGURE 37

```
SAE1006
LOW CARBON, HOT ROLLED
AISI 1006
PIETROWSKI, DOFASCO, OCT77
BHN 85



SAE1006      S1006B59     SHR     F1077
MOD = 30023.     YLD 0.2%= 36.     ULT.STR.= 46.
K= 60.     N= .145
BHN= 85.  %RA= 73.    SF=     0.    EF= 0.00
```

Figure 38 - Physical properties - materials file number 77.

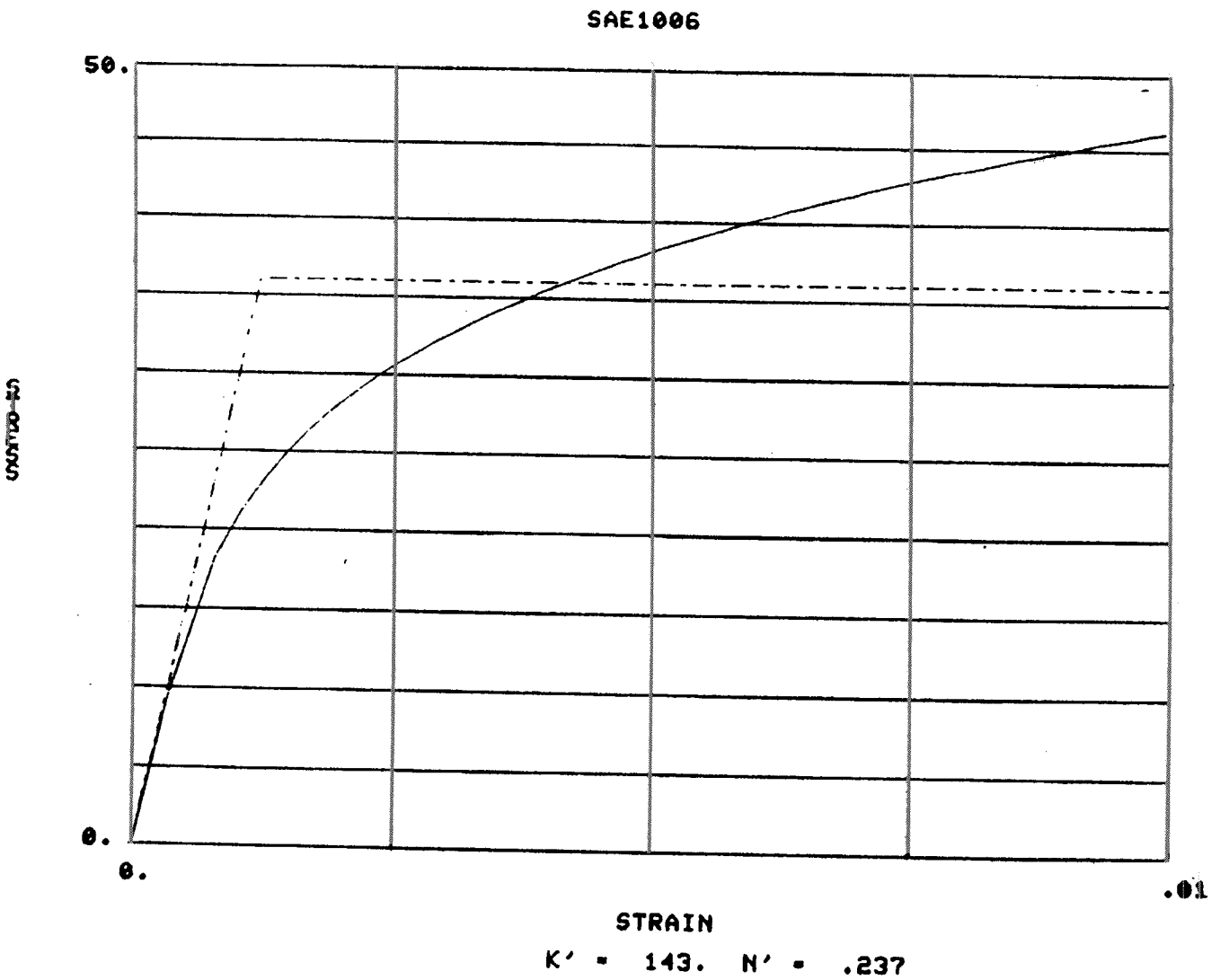


Figure 39 - Stress/Strain curve for materials file number 77.

| STRAIN | STRESS |
|---|---|
| .0 | .0 |
| .00063 | 15,176 |
| .00125 | 23,001 |
| .0025 | 30,612 |
| .00375 | 34,894 |
| .005 | 38,110 |
| .00625 | 40,790 |
| .0075 | 43,041 |
| .00875 | 44,863 |
| .01 | 46,364 |

DIGITIZED STRESS/STRAIN DATA - MATERIALS FILE NUMBER 77

FIGURE 40

```
SAE1006
AISI 1006
LOW CARBON,  HOT ROLLED
PIETROWSKI,  DOFASCO,  OCT77
BHN 85



SAE1006      S1006A59     SHR     F1078
MOD - 30023.     YLD 0.2%-  36.     ULT.STR.-  46.
K-  60.     N-  .145
BHN-  85.  %RA- 73.    SF-     0.    EF- 0.00
```

Figure 41 - Physical properties - materials file number 78.

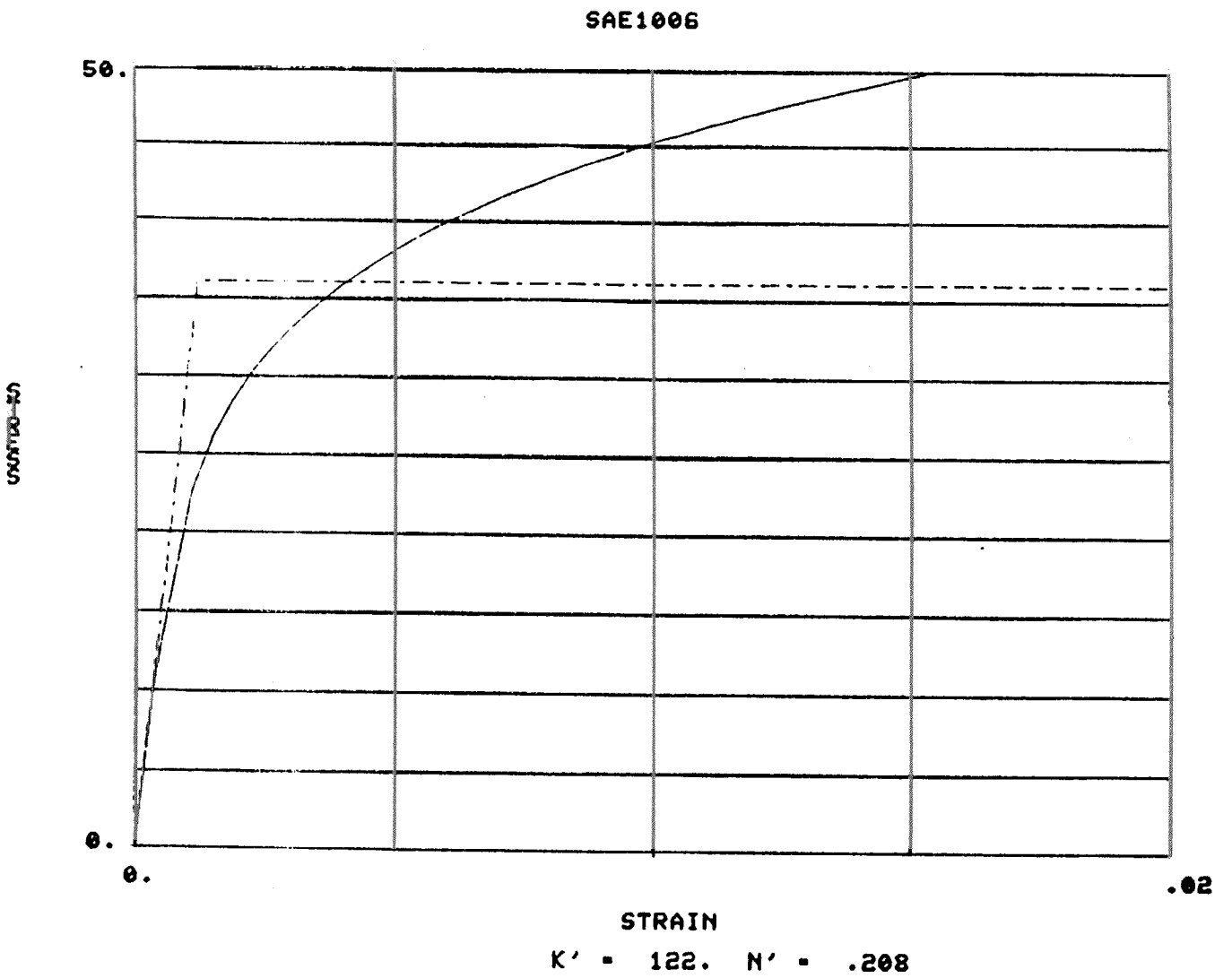


Figure 42 - Stress/Strain curve for materials file number number 78.

| STRAIN | STRESS |
|---|---|
| .0 | .0 |
| .00125 | 25,108 |
| .0025 | 31,346 |
| .005 | 38,441 |
| .0075 | 42,207 |
| .01 | 45,433 |
| .0125 | 47,798 |
| .015 | 49,949 |
| .0175 | 52,100 |
| .02 | 54,250 |

DIGITIZED STRESS/STRAIN DATA - MATERIALS FILE NUMBER 78

FIGURE 43

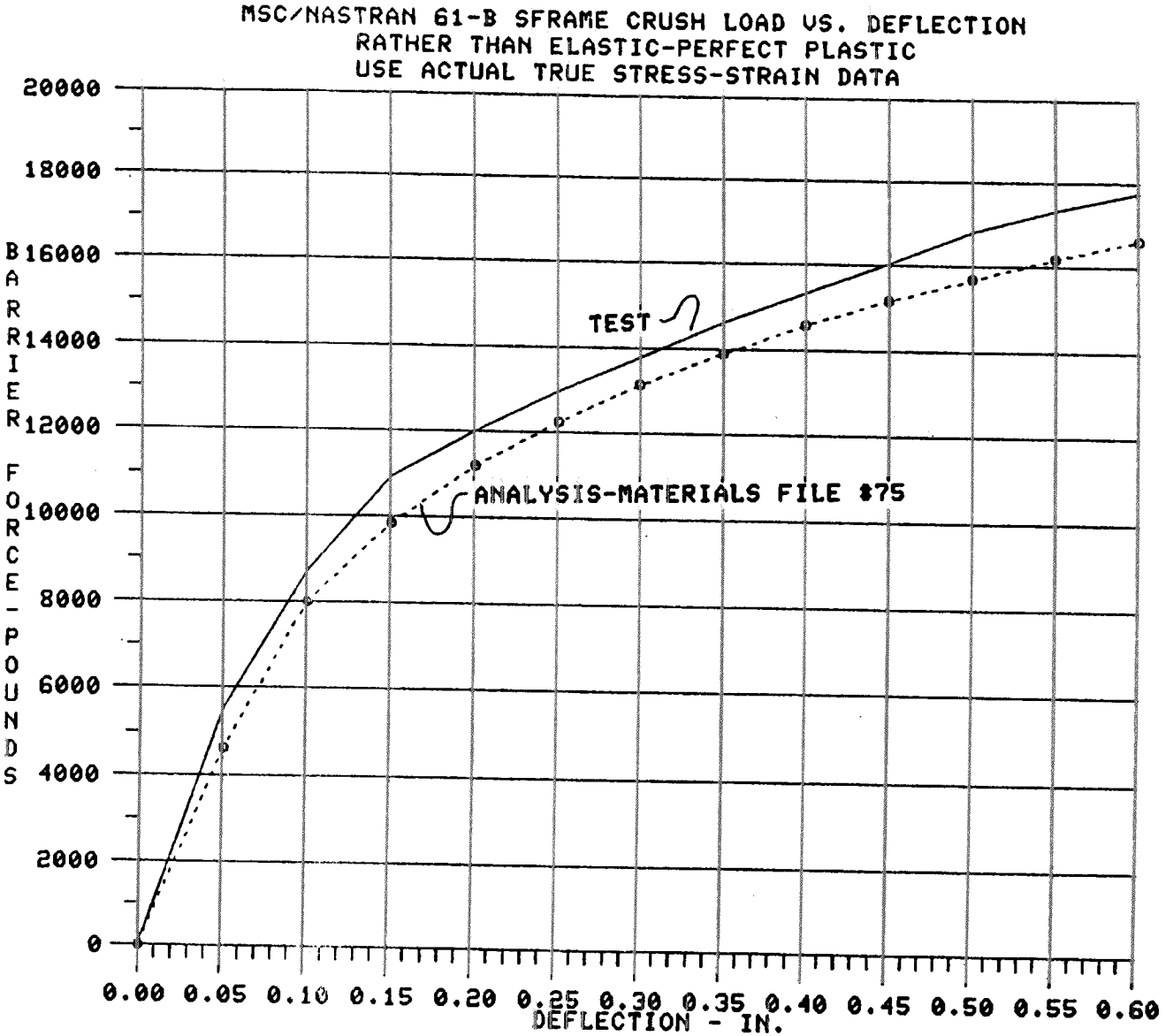


Figure 44 - Final Barrier Force versus Crush Distance curve - materials file number 75.

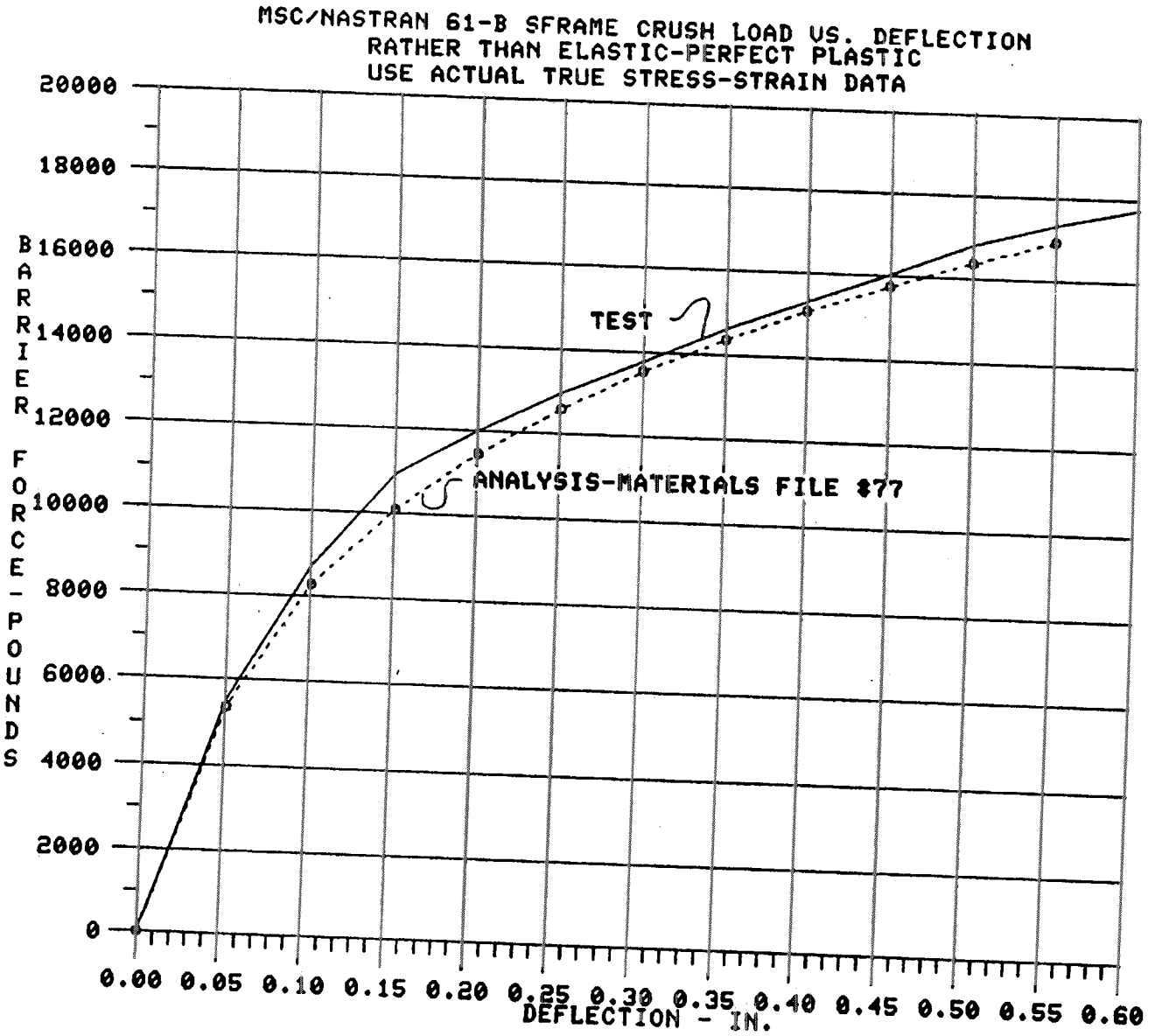


Figure 45 - Final Barrier Force versus Crush Distance curve - materials file number 77.

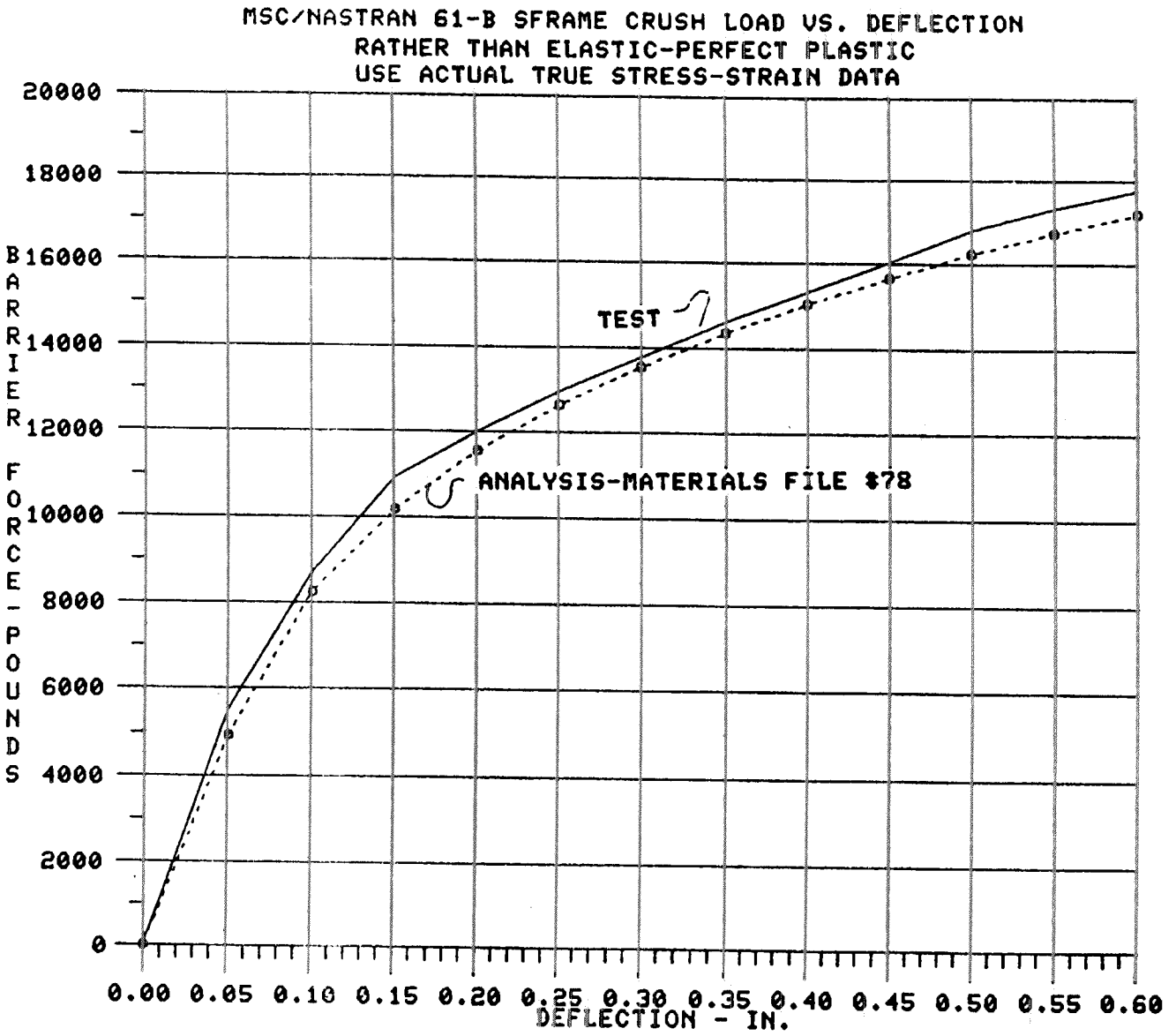


Figure 46 - Final Barrier Force versus Crush Distance curve - materials file number 78.

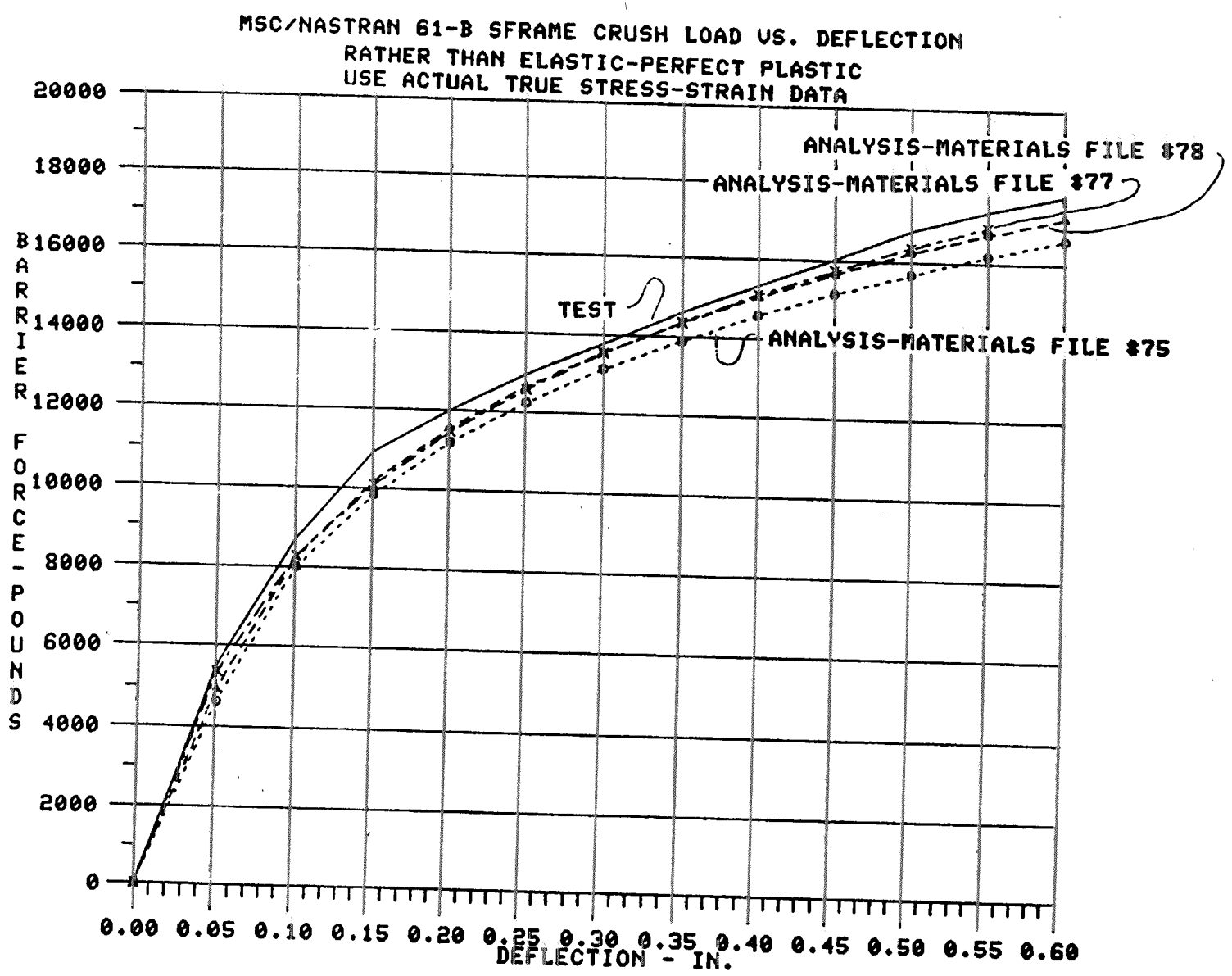


Figure 47 - Final Barrier Force versus Crush Distance curve - composite of 3 materials - Files 75, 77 & 78.

## REFERENCES


SAE 770614 - Elastic-Plastic Finite Element Analysis of Vehicle Structural Components; David S. Fine, Chevrolet Engineering Center, General Motors Corporation.

RN-372 - Application of "PLANS" Analyses to Nonlinear Structural Test Problems; Eileen Yander, Materials and Structural Mechanics Group, Grumman Aerospace Corporation.

SR-80-54 - WRECKER-F - General Purpose Nonlinear Finite Element Computer Program for Use in Automotive Crashworthiness Analysis; K. S. Yeung, Metallurgy Department, Scientific Research, Ford Motor Company.

SAE 810232 - Crush Strength Analysis of Lightweight Vehicle Frame Components; C. M. Ni, Engineering Mechanics Department, General Motors Corporation.

Light Truck Engineering Program Report - Belleville Spring Analysis; George Campbell, Light Truck Design Analysis (January 14, 1983)

Private communication with James Brancheau (June 15, 1982)

DISTRIBUTION LIST

STATIC GEOMETRIC AND MATERIAL NON-LINEAR ANALYSIS OF AN S-FRAME USING MSC/NASTRAN

S. M. Frey
C. L. Knighton
L. C. Veraldi

M. P. Anderson
K. H. Arning
D. J. Barrett
G. F. Bolling (6)
H. F. Cromwell
J. F. D'Aprile
F. Franz
H. P. Freers
J. E. Gilson
A. L. Gutherie
H. C. Jones
E. W. Kitzner
J. S. Logan
C. L. Magee
R. J. Marshall
D. T. Mullaney
H. W. Potoczak
N. J. Pritula
C. E. Scheffler
W. K. Slack
W. C. Tyner
H. F. Voigt
T. J. Walsh

File

Ford Library (1)

2/15/84)